AFRL-RX-WP-TP-2012-0389

MICROSTRUCTURE-SENSITIVE HCF AND VHCF SIMULATIONS (PREPRINT)

Craig Przybyla
Metals Branch
Structural Materials Division

William Musinski, Gustavo Castelluccio, and David L. McDowell
Georgia Institute of Technology

AUGUST 2012
Interim

AIR FORCE RESEARCH LABORATORY
MATERIALS AND MANUFACTURING DIRECTORATE
WRIGHT-PATTERSON AIR FORCE BASE, OH 45433-7750
AIR FORCE MATERIEL COMMAND
UNITED STATES AIR FORCE

REPORT DOCUMENTATION PAGE

Form Approved
OMB No. 0704-0188

1. REPORT DATE *(DD-MM-YY)*	2. REPORT TYPE	3. DATES COVERED *(From - To)*
August 2012	Technical Paper	1 July 2012 – 1 August 2012

4. TITLE AND SUBTITLE
MICROSTRUCTURE-SENSITIVE HCF AND VHCF SIMULATIONS (PREPRINT)

5a. CONTRACT NUMBER
In-house

5b. GRANT NUMBER

5c. PROGRAM ELEMENT NUMBER
62102F

6. AUTHOR(S)
Craig Przybyla (AFRL/RXCM)
William Musinski, Gustavo Castelluccio, and David L. McDowell (Georgia Institute of Technology)

5d. PROJECT NUMBER
4347

5e. TASK NUMBER
20

5f. WORK UNIT NUMBER
X071

7. PERFORMING ORGANIZATION NAME(S) AND ADDRESS(ES)
Metals Branch (AFRL/RXCM)
Structural Materials Division
Air Force Research Laboratory, Materials and Manufacturing Directorate
Wright-Patterson Air Force Base, OH 45433-7750
Air Force Materiel Command, United States Air Force

8. PERFORMING ORGANIZATION REPORT NUMBER
AFRL-RX-WP-TP-2012-0389

9. SPONSORING/MONITORING AGENCY NAME(S) AND ADDRESS(ES)
Air Force Research Laboratory
Materials and Manufacturing Directorate
Wright-Patterson Air Force Base, OH 45433-7750
Air Force Materiel Command
United States Air Force

10. SPONSORING/MONITORING AGENCY ACRONYM(S)
AFRL/RXCM

11. SPONSORING/MONITORING AGENCY REPORT NUMBER(S)
AFRL-RX-WP-TP-2012-0389

12. DISTRIBUTION/AVAILABILITY STATEMENT
Approved for public release; distribution unlimited. Preprint to be submitted to International Journal of Fatigue.

13. SUPPLEMENTARY NOTES
The U.S. Government is joint author of this work and has the right to use, modify, reproduce, release, perform, display, or disclose the work. PA Case Number and clearance date: 88ABW-2012-0613, 10 February 2012. This document contains color.

14. ABSTRACT
This paper provides some background and historical review of how microstructure-sensitive finite element simulations can play a role in understanding effects of stress amplitude, R-ratio, and microstructure on fatigue crack formation and early growth at notches, including pores and non-metallic inclusions for Ti alloys and Ni-base superalloys. Fatigue indicator parameters (FIPs) are computed over finite volumes that relate to processes of fatigue crack formation and early growth at the scale of individual grains. It is argued that both coarse scale (uncracked, mesoscale) and fine scale FIPs (computed in the vicinity of cracks in single grains or crystals) can be related to the cyclic crack tip displacement that serves as a driving force for crystallographic fatigue crack growth, and that the fine scale FIPs correlate directly with cyclic crack tip displacement. Scatter in HCF and VHCF is computationally assessed using multiple statistical volume elements and the distribution of FIPs of extreme value character. The concepts of marked correlation functions and weighted probability density functions are reviewed as a means to quantify the role of multiple microstructure...

15. SUBJECT TERMS
high cycle fatigue; fatigue indicator parameters; extreme value; microstructurally small cracks, modeling and simulation

16. SECURITY CLASSIFICATION OF:			17. LIMITATION OF ABSTRACT:	NUMBER OF PAGES	19a. NAME OF RESPONSIBLE PERSON (Monitor)
a. REPORT	b. ABSTRACT	c. THIS PAGE			Andrew Rosenberger
Unclassified	Unclassified	Unclassified	SAR	44	19b. TELEPHONE NUMBER *(Include Area Code)* N/A

Microstructure-Sensitive HCF and VHCF Simulations

Craig Przybyla[3], William Musinski[1], Gustavo Castelluccio[1], and David L. McDowell[1,2]

[1]Woodruff School of Mechanical Engineering
[2]School of Materials Science and Engineering
Georgia Institute of Technology, Atlanta, GA 30332-0405 USA

[3]Materials and Manufacturing Directorate, Air Force Research Laboratory
Wright-Patterson AFB, OH USA

ABSTRACT

This paper provides some background and historical review of how microstructure-sensitive finite element simulations can play a role in understanding effects of stress amplitude, R-ratio, and microstructure on fatigue crack formation and early growth at notches, including pores and non-metallic inclusions for Ti alloys and Ni-base superalloys. Fatigue indicator parameters (FIPs) are computed over finite volumes that relate to processes of fatigue crack formation and early growth at the scale of individual grains. It is argued that both coarse scale (uncracked, mesoscale) and fine scale FIPs (computed in the vicinity of cracks in single grains or crystals) can be related to the cyclic crack tip displacement that serves as a driving force for crystallographic fatigue crack growth, and that the fine scale FIPs correlate directly with cyclic crack tip displacement. Scatter in HCF and VHCF is computationally assessed using multiple statistical volume elements and the distribution of FIPs of extreme value character. The concepts of marked correlation functions and weighted probability density functions are reviewed as a means to quantify the role of multiple microstructure attributes that couple to enhance the extreme value FIPs in the HCF regime. An algorithm for estimation of the cumulative probability distribution of cycles for crack formation and growth from notches in HCF and VHCF is also described.

1. Background and Objectives of Microstructure-Sensitive Fatigue Modeling

Quantifying variability of fatigue life in the HCF and VHCF regimes is a common goal to support design based on low probability of failure and typically requires extensive and time consuming experimental studies. We primarily consider here the effects of microstructure on fatigue variability of Ti alloys and Ni-base superalloys, advanced alloys used in aircraft gas turbine engine components. The goal of microstructure-sensitive polycrystal plasticity simulations is to assist in reducing the number of experiments required by developing computational schemes that can be used to help design, analyze and qualify new microstructures that are more fatigue resistant for a given application. Specifically, the intent is to characterize the influence of microstructure on fatigue life variability under constant amplitude loading conditions, with particular attention to the shape of the low cumulative probability tail regions. An added benefit is a direct pathway to identifying mesoscale microstructure attributes, either by themselves or via coupling amongst multiple attributes, that contribute to "hot spot" neighborhoods with high probability form fatigue cracks.

The focus of the present state-of-the-art is on the role played by mesoscale arrangement of grains and phases, encompassing various spatial statistics including orientation and disorientation distributions [1]. While variability also may arise from the nanoscopic scale in association with crack nucleation mechanisms, it is useful to consider that much of the observed variability in polycrystalline systems arises from microstructure at scales well above 1 μm, considered here as scale representative of embryonic stage of crack formation. The origins of these kinds of mesoscopic simulations of heterogeneous materials to understand the role of microstructure and related stochastic/probabilistic aspects with applications to

various responses and/or properties can be traced back to the early to mid-1980s with the advent of computational micromechanics. For example, Asaro [2], Asaro and Needleman [3], McHugh et al. [4], and Deve et al. [5] developed early polycrystalline finite element models for shear localization in polycrystalline microstructures with ductility and strength in mind. Needleman and colleagues [6-7] considered the growth of grain boundary cavities and interactions of fibers with matrix material using finite element methods in the process of nucleation and growth of voids. Needleman [8] extended these approaches to address interfacial failure in finite element models of idealized or actual microstructure representations using cohesive zone methods. By the early 1990s considerable efforts were underway in computational mesoscopic modeling of microstructure-property relations directed towards various classes of heterogeneous materials. Extending earlier works of Asaro, Needleman and colleagues, Zikry [9-11] considered the effects of crystallite orientation distribution and grain boundary network on failure modes in large scale computational crystal plasticity using finite element methods.

The integration of computational micromechanics with probabilistic failure descriptions was a natural outcome of the rapid development of the field of computational micromechanics in the 1980s. Haddad (1990) considered the effect of microstructure on distribution of slip in polycrystals. The work of Chamis and colleagues [13] at NASA integrated the notions of computational micromechanics simulation of heterogeneous materials (composites) with probabilistic analyses to advocate low probability of failure design methods for different failure modes. Duva et al. [14] and Ruggieri and Dodds [15] employed computational simulations of heterogeneous materials and cracked to support probabilistic computational micromechanics characterization of damage evolution.

Appealing to much earlier work on stochastic deformation and failure of random heterogeneous materials (cf. Krajcinovic [16]), and in recognition of the expense of finite element methods, lattice-spring methods were used by Ostoja-Starzewski et al. [17] to characterize probability distributions of damage evolution in random heterogeneous materials. Zhou and Zhai [18-19] built on the earlier works of Needleman to model dynamic fracture of realistic microstructures by placing cohesive zone elements between all elements in explicit finite element simulations, including effects of distribution of interface cohesive strength and energy. Variability of response (e.g., crack growth history) is a natural outcome of such simulations.

Early works in fatigue of heterogeneous materials were typically focused on composite micromechanics [20-23]. Even earlier works in mesoscopic simulations of metallic polycrystals for purposes of characterizing distributions of driving forces for fatigue crack formation can be traced to early works of Provan [24-25], Cox and Morris [26] and Sakai et al. [27]. The interaction of small cracks with microstructure and related mesoscopic models for crack growth in random microstructures had been understood and modeled in the 1980s (cf. Monte Carlo simulations by Tanaka and Akiniwa [28] with random microstructure that correctly predict the magnitude of scatter of the small crack *da/dN* using a simple $da/dN = A(ACTOD)^m$ relation, where ACTOD is the range of crack tip opening displacement). McDowell [29] reviewed the status of microstructure sensitivity to formation and growth of small cracks in HCF. Gall et al. [30] used finite element simulations to study the effects of crystallographic orientation on variability of microstructurally small crack growth rate in crystals using CTOD concepts.

The mesoscopic modeling of distributed crack formation within grains of a polycrystalline ensemble by Hoshide and Socie [31] that employed slip band cracking models and crack growth relations was a precedent in motivating the later work in the field; all essential elements of crack nucleation in slip bands in grains and early growth were treated for metallic polycrystals with the approximation of Sachs (isostress) among grains. McDowell [32] discussed the importance of such mesoscopic simulations to understand fatigue phenomena. This work clarified that for fatigue the notion of a statistically homogeneous representative volume element (RVE) is problematic; many practical cases it is too large to be relevant to actual specimens or structures, particularly in the HCF regime. This had been stressed earlier in the work of Lacy et al. [33] which showed that the RVE size for elastic stiffness of a field of microcracks in a brittle material (e.g., polycrystalline ceramics) is much too small to be considered as a RVE for the evolution of damage. According, it is necessary to build up statistics based on multiple computational realizations [34] of smaller statistical volume elements (SVEs) to arrive at a proper

statistical distribution of responses, or to employ approaches that weight input from SVEs to achieve much more efficient characterization of ensemble statistics [35-36]. In other words, it is not appropriate to select a size for a computational volume of a heterogeneous material by considering convergence of the average stress-strain behavior or elastic stiffness if fatigue crack formation and growth are the relevant responses. The notion of a RVE implies that even the higher order moments of the statistical distribution of fatigue driving forces are fully captured, not just the lowest order, the point made earlier in reference to evolving damage [33] and fatigue [34].

The PhD thesis of Bennett [37] and derived papers by Bennett and McDowell [38-41] used finite element models with crystal plasticity to compute distributions of slip and projected distributions of fatigue cracks in polycrystals based on multiple realizations of a nominal microstructure. In addition, they computed the cyclic crack tip displacement range (both opening and sliding components) as a function of crack length relative to grain size from surfaces in polycrystals. In the DoE USCAR program from 1995-2000, McDowell and colleagues [42-46] employed finite element modeling at the scale of microstructure to model formation and early growth of interdendritic cracks in A356-T6 casting alloys, culminating in the formulation of a probabilistic framework for fatigue response based on various distributions of microstructure attributes at five different length scales of attributes. During the same time period, Tryon and Cruse [47-49] related the notion of mesoscopic modeling of microstructure to reliability within the context of finite element simulations of polycrystalline microstructures.

The past decade has witnessed a significant increase in attention devoted to mesoscopic modeling of cyclic deformation processes at the microstructure scale. In addition to the scheme outlined in the next section, recent works in this regard by Dunne and colleagues [50-55] and Ghosh and co-workers [56-59] are noted.

2. FIP Methodology

Microstructure-sensitive crystal plasticity modeling methods have rapidly developed within the past decade [1,46,60-62]. The basis for these methods is consideration of effects of microstructure morphology (size, shape, orientation/disorientation, and spatial statistics of grains/phases) on the distribution of cyclic and directional slip and local stress states in 3D microstructures to quantify the probability of forming and growing small fatigue cracks [31,60-61,63-64]. The methodology supports the notion of design of microstructures to enhance fatigue resistance in DOE USCAR [46], DARPA AIM [65-68], and DARPA Prognosis [69] and related programs [70] that have utilized this kind of strategy to address sensitivity of fatigue crack formation to microstructures of engine materials (Ni-base superalloys and α–β Ti alloys in the engine systems prognosis program).

The primary modeling "workhorse" of these methods has been computational crystal plasticity, which serves to identify and characterize local material hot-spots controlled by intrinsic (e.g., local grain orientations) or extrinsic (e.g., inclusions or large precipitate) microstructure attributes. McDowell [29,60-61] has discussed in-depth the utility of crystal plasticity in sensitivity studies that support design of microstructure morphology (heat treatment, thermo-mechanical processing) for fatigue resistance, with emphasis on variability in fatigue life in the high cycle fatigue regime. The key elements of this approach are the identification of key fatigue damage modes at the scale of grains and assignment of corresponding nonlocal (volume averaged) Fatigue Indicator Parameters (FIPs). These elements are employed in the estimation of expected initial crack distributions based on assumed nucleation and growth relations at the scale of grains, and limited small crack growth simulations within heterogeneous microstructure. Different FIPs [1,61-62] have been introduced to reflect the relative roles of reversed and cumulative directional slip at the scale of individual grains or crystalline regions in polycrystals (i.e., microplasticity) on driving formation of cracks, either transgranular along slip bands or intergranular due to progressive slip impingement, as shown in Figure A1. In high cycle fatigue (HCF), the majority of component life is typically spent in processes of forming and growing cracks in the microstructurally small crack (MSC) regime, with crack sizes on the order of characteristic microstructure length scales (grain size, phase or cluster spacing or diameter). For example, the Fatemi-Socie [71-72] shear-based FIP (two parameter

approach) has been shown to correlate multiaxial fatigue crack initiation data very well in both LCF and HCF regimes at the grain scale and above [63,73-74]. It is defined by

$$FIP_{FS} = \frac{\Delta\gamma^{p*}_{\max}}{2}\left(1 + K\frac{\sigma^{n*}_{\max}}{\sigma_y}\right) \tag{1}$$

where $\Delta\gamma^{p*}_{\max}/2$ is the nonlocal maximum cyclic plastic shear strain averaged over a finite volume of material (on the order of several μm^3), $\sigma^{n*}_{\max}$ and σ_y are the maximum stress normal to the plane of $\Delta\gamma^{p*}_{\max}/2$ and cyclic yield strength, respectively, and constant K mediates the influence of normal stress. The spatial volume for nonlocal averaging of the FIP may be defined according to the nature of the simulation, and is desirable both for purposes of numerical regularization (mesh insensitivity) and targeting length scales associated with crack embryos (e.g., slip band width/spacing, inclusion size, etc.). A similar but distinct parameter has been introduced by McDowell [61] to address correlations of directional plastic strain accumulation with crack formation due to grain or phase boundary impingement (Zener pileup), i.e.,

$$FIP_{ZP} = \gamma^{p*}_{net}\left(1 + K_z\frac{\sigma^{n*}_{GB}}{\sigma_y}\right) \tag{2}$$

where $\gamma^{p*}_{net} = \max\left(n_i\varepsilon^{p*}_{ij}m_j\right)$ is the maximum net plastic shear strain averaged over a finite volume of material among all planes with unit tangent and normal vectors **m** and **n**, respectively, σ^{n*}_{GB} is the average peak stress normal to a boundary segment impinged by this slip, and K_z is a constant that mediates the effect of this normal stress. This kind of directional (or ratchet) strain accumulation is key to understanding rolling contact fatigue processes within heterogeneous microstructures consistent of grains of various sizes, shapes and orientations and nonmetallic inclusions, of high relevance to life-limiting situations in bearing applications, for example.

The philosophy of this mesoscopic approach to fatigue lifetime prediction and characterization of variability of multiple stages of crack nucleation and growth has been elucidated in recent reviews by McDowell [61-62] and McDowell and Dunne [1]. McDowell and colleagues [77] have developed schemes by which microstructure-sensitive polycrystal plasticity models for duplex Ti-6Al-4V [78-81], $\gamma-\gamma'$ Ni-base superalloys [82-83], and martensitic steels [84-86] can be analyzed in terms of distributions of slip and mechanism-relevant continuum FIPs, including effects of pores and nonmetallic particles on initiation of fatigue cracks. When employed in the context of polycrystal plasticity, these FIPs enable assessment of the relative potency to nucleate and grow cracks at the scale of individual grains by assigning a relation between the number of cycles necessary to nucleate a crack at the scale of the nonlocal averaging volume and the associated FIP, i.e., $N_{nucl} = f(FIP)$, for example using an extension of a slip band-based nucleation criterion [83].

The methodology has also been extended to a multistage decomposition of the total fatigue life given by McDowell et al. [46,60-62], i.e.,

$$N_T = N_{nucl} + N_{MSC/PSC} + N_{LC} \tag{3}$$

where N_{nucl} is the number of cycles necessary to form a crack embryo at scales on the order of microns, $N_{MSC/PSC}$ is the number of cycles necessary to grow microstructurally/physically small cracks through the adjacent microstructure, and N_{LC} is the number of cycles of growth of mechanically long cracks that meet similitude requirements of Linear Elastic Fracture Mechanics (LEFM). Typically, fatigue crack nucleation occurs crystallographically within a favorably oriented grain/phase, particularly for low to moderate stacking fault energy fcc crystals or hcp crystals with a tendency towards planar slip. A useful

heuristic is to use grain level FIPs to project cycles to form at crack at the scale of individual grains or phases, often tens of microns in size, which is a combination of nucleation and microstrrucTurally small crack (MSC) growth phases, i.e., the incubation life $N_{inc} = N_{nucl} + N_{MSC}\big|_{first\ grain}$.

Shenoy et al. [83] have also applied a MSC regime growth law for Stage I crystallographic growth that employs the two –parameter FIP in Eq. (1) (sliding displacement controlled by cyclic plastic shear strain, with an additional effect of peak normal stress to this plane), where the analogy to mixed mode ΔJ-integral [87] and cyclic crack tip displacement range ΔCTD is made (cf. [88]), i.e.,

$$\left.\frac{da}{dN}\right|_{MSC} = A_{FS}\left(\tau_y FIP_{FS}\right)a - \eta_i b = \phi\,\Delta CTD - \eta_i b \tag{4}$$

where A_{FS} is a constant, τ_y is the critical resolved shear stress on the slip plane, and ΔCTD_{th} is a threshold crack tip displacement range below which the crack will not grow. Clearly, relation (4.1) employs a FIP that is averaged over an uncracked domain of a grain or phase as a driving force parameter when multiplied by crack length that is intended to parameterize the dependence of the fine scale propagation relation in (4.2) on ΔCTD. Later discussion will shed light on the implied connection of the quantity $\left(\tau_y FIP_{FS}\right)a$ to ΔCTD. In Eq. (4), an equivalence of the middle relation in (4.1) is implied with regard to the relation based on ΔCTD via the right expression (4.2), where b is the magnitude of the Burgers vector and ϕ and is an irreversibility factor that controls cyclic crack advance associated with the fraction of process zone dislocations that do not return to the crack tip during unloading. Parameter ϕ carries the "imprint" of atomic scale processes of new crack surface creation owing to slip irreversibilities and can effects of interactions with precipitates and impurities. The threshold $\eta_i b$ characterizes the level of irreversible range of the ΔCTD below which the crack should not extend, with η_i on the order of unity.

This methodology considers the sequential processes of crack formation in hot spot grains during cyclic loading and growth through multiple adjacent grains, with no attempt to resolve mechanisms in the sub-micron scale regime related to incipient stages of crack formation/nucleation. Accordingly, it is argued that microstructure at scales of microns and above, including size, shape and spatial distributions of grains/phases, orientation and misorientation effects, and extrinsic attributes such as nonmetallic inclusions or pores, has a dominant influence on the variability of HCF and VHCF fatigue life, which is spent dominantly within the regimes of initial crack formation and growth in the surrounding few grains/phases. For this reason, the algorithms in the present paper do not consider crack growth into the physically small and long crack regimes.

Under HCF conditions, the cyclic plastic deformation is highly heterogeneous within the microstructure; accordingly, this is the regime in which variability and size effects are most pronounced. A strategy for computational HCF modeling of components that must last millions of cycles, such as shafts, bearings, and gears, for example, should focus on extreme value statistics of potential sites for microplastic strain localization and fracture that drive crack formation and early growth. Moreover, the issue of arrest of small cracks that form at isolated sites of cyclic plastic strain intensification with in the microstructure is relevant to fatigue strength thresholds. There are several types of thresholds [89]. One is the absence of microplasticity within grains sufficient to nucleate cracks or to drive growth of micron-scale embryonic cracks within individual grains/phases. Another somewhat higher threshold is associated with crack arrest at either the first or second major impediment to slip, typically either grain or phase boundaries. The latter is commonly referred to as a non-propagating threshold or fatigue limit, and is relevant to HCF conditions. The realm of thresholds in VHCF is relatively unexplored, and it is interesting to consider that a change of deformation mechanism or dislocation substructures at these lower cyclic plastic strain levels may give rise to thresholds for which we have little understanding at present.

Prediction of effects of variable amplitude load histories and prediction of mean fatigue life as a function of microstructure are objectives with added complexity and are presently beyond the purposes and scope of the class of approaches considered here. In fact, true prediction of mean fatigue life requires

complete understanding of crack nucleation processes, which involve dislocation substructures and mechanisms at the nanoscale, including specific effects of composition, solid solution strengthening, etc. Fatigue crack nucleation is indeed a grand challenge problem, since it considerable idealization may be involved. Very recent works of Sangid et al. [90-91] are promising in this regard and consider not only the grain orientation distribution but also address the grain boundary character distribution using energetic approaches for nucleation that essentially lend more physics to earlier concepts of dislocation dipole models for crack nucleation by Tanaka and Mura [92] and Venkarataman et al. [93] that combine slip banding with an energetic description. They have also demonstrated the ability to project variability of HCF life for a polycrystalline ensemble. We note, however, that there are yet unresolved questions regarding the role of vacancies in the emergent instability of a crack forming in a lattice. Work in the role of generation of point defects (mainly vacancies) due to production and annihilation of dislocations within regions of localized cyclic plastic deformation goes back several decades [94-96]. Using positron annihilation, Egger et al. [97-98] have shown that vacancy concentration evolves in fatigue (but not monotonic fracture) within regions of localized slip to the point at which cracks nucleate. The significance of these studies is that the driving force for crack nucleation is affected by the production and migration of point defects and not just based on dislocation pileups, as proposed by Tanaka and Mura [92].

For the time being, we proceed in microstructure-sensitive design of advanced alloys without explicit *predictive* models for nucleation, owing to the role of microstructure in affecting small fatigue crack growth and inducing fatigue limits through blockage of small cracks. This can be augmented in time gaining a more predictive footing with regard to crack nucleation processes. Of course, an interesting question is what minimal set of microstructure information is necessary to predict variability of fatigue life for a given microstructure and loading condition. It is not fully resolved, but suffice it to say that attention is drawn to the life limiting features in HCF such as largest favorably oriented grains, adjacent grains with favorable orientation, interactions among grains that enhance slip, nonmetallic inclusions at higher scales, etc. Mesoscale simulations of the type considered here can provide much useful information even in the absence of predictive nucleation relations that reflect composition and grain boundary character.

Quantifying the sensitivity of fatigue life to microstructure opens several avenues:

- The ability to tailor microstructure to improve fatigue resistance
- Comparison of candidate microstructures for specific applications, including low probability of failure regimes of interest to design applications
- The ability to augment costly experiments in the HCF and VHCF regimes to quantify variability and scatter in fatigue

This paper will consider mainly the latter two items in the list above. However, they enable the first one, namely providing decision-support for tailoring microstructure to achieve enhanced fatigue resistance. Figure 2 shows a loop in microstructure design that employs the microstructure-sensitive simulation methods outlined here. By subjecting digital statistical volume elements (SVEs) constructed in adherence with spatial statistics of actual microstructures to computational simulation for representative loading histories, a distribution of microstructure (e.g., grain) scale FIPs are computed for many SVEs and the histogram used to assess the range of expected minimum fatigue lives for a given nominal microstructure and loading condition. This information is then fed back into the instantiation of digital SVEs with modified microstructure aimed at increasing minimum life or reducing variability, according to design targets. There are several potential design applications of this kind of approach. For example, (i) designing application-specific composition and process route, (i) grading microstructures in components (location specific properties), and (iii) accelerating certification of design for minimum life.

Within this paradigm, there are several important points. First, it is assumed that variability emerges mainly from the state of cyclic inelastic deformation within individual grains/phasees, which is affected primarily by grain size, shape, orientation and relation to/coupling with neighboring grains. This is particularly important in HCF since only favorable grains are activated within a highly heterogeneous

field. Second, the constitutive models for deformation and for relating FIPs to lifetime estimates should be calibrated to mean fatigue response of specific microstructures (validation), for several reasons:

- uncertainty in idealization and approximation of models (e.g., slip, nucleation, crack growth)
- potential omission of deformation or fatigue damage mechanisms

It may seem counter-intuitive but absolute prediction of fatigue life is well beyond current capabilities of this kind of modeling framework until relations for fatigue crack nucleation and microstructurally small crack growth are better understood and quantified. When mean fatigue response is used to calibrate models for a given fatigue loading condition and set of microstructures, so long as the dominant mechanisms don't change, it is assumed that mean fatigue responses can be projected for the same loading conditions and other microstructures within the range calibrated or modeled.

3. Multiaxial Fatigue and FIPs

One of the primary motivating features for using FIPs is their simplicity as computable mesoscopic parameters, while demonstrating desirable predictive character for multiaxial stress/strain states of the kind that grains/phases actually experience. A wide-range of FIPs have been proposed in the last 30 years to characterise the formation and early growth of fatigue cracks. Socie and Marquis [100] summarized many of the FIPs devised on stress, strain or energy concepts, which supports that a single continuum parameter cannot correlate equally well with the multiaxial fatigue crack initiation behavior of all metals. For example, the FIP proposed by Fatemi and Socie [71] in Eq. (1) based on the critical plane approach correlates well with the small fatigue crack formation and growth in ductile metals that sustain shear-based fatigue damage.

3.1 Coarse Scale (Uncracked) FIP Correlations for Multiaxial Fatigue

As suggested by Reddy et al. [101] and McDowell and Berard [88], the Fatemi-Socie FIP can be understood as a local fatigue driving force similar to the ΔK or the ΔJ customized to describe the early crystallographic crack growth phenomena. Indeed, McDowell and Berard [88] and McDowell [63] showed that the Fatemi-Socie parameter in Eq. (1) resulted in fatigue life correlations over a broad range of multiaxial loading conditions in a manner similar to small fatigue crack growth relations motivated by the ΔJ -integral of Elastic-Plastic Fracture Mechanics (EPFM). Hoshide and Socie [87] appealed to the elastic and plastic forms of the standard *J*-integral expression of EPFM to model mixed mode crack growth in multiaxial fatigue, with *J* given by

$$J = \frac{\pi\left(\sigma^2 + \tau^2\right)}{E} a_{eff} + \tilde{J}\left(n, \lambda_\sigma, \xi_\sigma\right) \overline{\sigma}\overline{\varepsilon}^p a = J_e + J_p \tag{5}$$

Here, a and a_{eff} are actual and effective crack lengths, and the stress biaxiality ratios are given by $\lambda_\sigma = \tau / \sigma_{yy}$ and $\xi_\sigma = \sigma_{xx} / \sigma_{yy}$, where τ and σ_{yy} are the far field shear and crack plane normal stresses, respectively, and σ_{xx} and is the direct stress parallel to the crack. Considering ΔJ for cyclic loading based on the loading part of the cycle, they correlated crack growth data for IN 718 for cracks less than 1 mm in length using the power law relation

$$\frac{da}{dN} = C_J \left(\Delta J\right)^{M_J} \tag{6}$$

where C_J and M_J depend on the biaxiality ratios, and M_J ranged from 1.31 to 1.45. It turns out that small crack growth data (crack lengths on order of hundreds of microns, beyond the follow reasonably

well this kind of correlation based on the homogeneous, macroscopic value of ΔJ (cf. McDowell, 1996HCF). This is perhaps not surprising owning to the linear relation between J and CTOD even under EPFM conditions [102].

By effectively asserting a coarse scale (based on uncracked cyclic plastic strain field) $\mathrm{FIP}_{\mathrm{FS}}$-based growth law of the type given in Eq. (4) for physically small cracks under plasticity-dominated LCF conditions, McDowell [63] showed that the characteristic contours for multiaxial fatigue in the so-called Γ^{p}-plane were in qualitative agreement with trends from experimental data, as shown in Fig. 3. The Γ-plane was introduced by Brown and Miller [103] and presents trajectories of constant fatigue life data corresponding to a crack of a given length, say 500 μm, in terms of maximum range of shear strain versus peak normal strain to the same plane. McDowell and Berard [88] introduced a more complex variant of this growth relation with more degrees of freedom to match experimental data for each of the two branches evident in Fig. 3.

Alternatively, when the nonlocal FIP is computed in the vicinity of the tip of a small crack, it includes the plastic strain intensification due to crack and the relation in Eq. (4) may written as

$$\left.\frac{da}{dN}\right|_{MSC} = A_{FS}^{'}\ \mathrm{FIP}_{\mathrm{FS,\ crack}}\ \bar{d} - \Delta\mathrm{CTD}_{th} \tag{7}$$

where $\bar{d}$ is a characteristic length scale employed for averaging the fine scale FIP. In this case, the product $\mathrm{FIP}_{\mathrm{FS,\ crack}}\ \bar{d}$ is intended to parameterize the $\Delta\mathrm{CTD}$; for this to hold, it must turn out that $\mathrm{FIP}_{\mathrm{FS,\ crack}}$ is linearly related to $\Delta\mathrm{CTD}$. We will explore the efficacy of $\mathrm{FIP}_{\mathrm{FS,\ crack}}$ in Eq. (7) in the next section, with reference to driving force for crystallographic cracks in single crystals.

3.2 Microstructurally Small Crack Growth – Direct Relation of $\mathrm{FIP}_{\mathrm{FS,\ crack}}$ to ΔCTD

In this section we compare the Fatemi-Socie FIP with the damage-tolerant approaches (e.g., LEFM, EPFM) have traditionally estimated the fatigue crack growth driving force by means of the range of stress intensity factor (ΔK), the range of J-integral (ΔJ) or the range of crack tip displacement (ΔCTD). The experimental validation of these magnitudes is usually based on far-field measurements (an exception is Schwalbe's δ_5 [104]) that rely on the similitude assumption of fracture mechanics. However, as discussed by McDowell [29], the similitude assumption is often not valid when the crack length or cyclic plastic zone size is on the order of the characteristic dimensions of the microstructure. In this case, microstructure-sensitive characterizations need to consider local fields to estimate fatigue driving forces. Since the concept of a ΔCTD does not rely on the similitude hypothesis, it is a potential measure of the local crack driving force, but requires detailed FEM simulations to capture the influence of load sequence and microstucture in the vicinity of the crack tip. Recently, Castelluccio and McDowell [105-106] compared the fine scale Fatemi-Socie $\mathrm{FIP}_{\mathrm{FS,\ crack}}$ (i.e., computed within a cracked single grain or crystal) to the ΔCTD using finite element simulations of single crystals with cracks on {111} slip planes under shear and mixed mode loading. For simplicity, we omit the subscript for the remainder of this section and refer to $\mathrm{FIP}_{\mathrm{FS,\ crack}}$ simply as "FIP". They employed 3D crystal plasticity constitutive models within user material subroutines for the FE code ABAQUS [107] for both OFHC Cu and RR1000 Ni-base superalloy single crystals oriented for single slip in remote shear loading, with a sense parallel to the crack. A total of five models with stationary crack lengths of 2 μm, 5 μm, 7.5 μm, 10 μm and 15 μm were analyzed; Fig. 4 shows one example. The upper and lower faces of the crystal in Fig. 4 were cyclically displaced in shear or mixed mode loading, as shown in Fig. 5; three loading cycles were applied with the magnitude of the displacement vector **D** ranging from 0.005 μm to 0.1 μm, equivalent for this geometry to nominal peak strains from 0.05% to 1%. The strain ratio $R_{\varepsilon} = \varepsilon_{\min}/\varepsilon_{\max} = 0$ was employed, where $\varepsilon_{\max}$ and $\varepsilon_{\min}$ are the maximum and minimum applied strain over a loading cycle. For homogeneous single crystals, these

values resulted in plastic strain amplitudes that spanned the HCF to LCF regimes. The FIP was averaged in this case within a band of uniform 2 μm thickness parallel to the crack, as shown to the right in Fig. 4.

The ΔCTD was evaluated by measuring the displacement between red nodes in Fig. 4 at the mid-thickness over the loading portion of the third loading cycle. The total crack tip displacement range was calculated as

$$\Delta CTD=\sqrt{\Delta CTSD^2+\Delta CTOD^2} \tag{8}$$

based on the work of Ma et al. [108] and employed by Bennett and McDowell [39-41]. The cyclic crack tip opening (ΔCTOD) and sliding (ΔCTSD) displacements were computed based on the change in distance between red nodes shown in Fig. 4.

Because the ΔCTD includes elastic and plastic contributions, the FIP was calculated for each element based on the total strain tensor. Figure 6 compares the ΔCTD with the fine scale FIP for shear (left) and mixed mode (right) loading and OFHC Cu and RR1000 Ni- base superalloy. Even though the averaging volume was defined in terms of a band as shown in Fig. 4, Cu and RR1000 exhibit similar behavior with regard to the correlation of the fine scale FIP with ΔCTD under single slip shear loading. The correlation for Cu under mixed mode loading is nearly identical, whereas for the Ni-base superalloy there is increased variability for mixed mode loading. Results in Fig. 6 essentially demonstrate linearity of the ΔCTD with the FIP for both loading modes for ΔCTD values above 1 nm, which is on the order of the magnitude of the Burgers vector.

Hence, it is interesting to note that whether a coarse scale (uncracked) or fine scale (cracked) FIP_{FS} is employed, there is close respective connection to both multiaxial fatigue behavior of shear-dominated crack initiation (formation and early growth) processes at the mesoscale [63,88] and the ΔCTD driving force for crystallographic fatigue crack growth in single crystals. This suggests utility of the FIP concept from single grains to mesoscales involving many grains, regardless of whether similitude requirements of LEFM are met.

4. Microstructure Attributes and Extreme Value Correlations in HCF

4.1. Grains (size, shape, orientation, and disorientation distributions)

Grain size can have a significant effect on the fatigue failure mechanism in Ti alloys and Ni-base superalloys with a given microstructure. The grain boundary network is also relevant. Directionally solidified and single-crystal forms of Ni-base superalloys suppress or eliminate grain boundary diffusional creep and intergranular oxidation mechanism at elevated temperatures. The AIM program [65-67] hinted at the possibility of location specific design of components (e.g., dual or hybrid microstructures) with optimized microstructure to meet operational requirements (stress state, temperature, environment, etc.) in different regions of components.

The mode of fatigue crack formation and growth in Ni-base superalloys at elevated temperatures strongly depends on the grain size of the microstructure. For subsolvus, fine grain (average grain sizes ~ $3-15\mu m$) Ni-base superalloys, cracks tend to form via a Stage II, non-crystallographic, transgranular cleavage mechanism near non-metallic inclusions (NMIs) or pores [109-111]; this fatigue crack growth mechanism transforms to intergranular growth for surface cracks when the crack reaches a characteristic length ($\sim 50-100\mu m$) [109-111] or when dwell periods occur [110]; for sub-surface cracks, intergranular cracking requires crack lengths greater than the characteristic length and exposure of the crack to the surface [110]. Alternatively, due to the planar slip mechanism in Ni-base superalloys [111-112], supersolvus, coarse grain (average grain sizes $\geq 15\mu m$) Ni-base superalloys favor Stage I crystallographic crack formation from inclusions, pores or large grains. This fatigue mechanism has been observed in Rene' 88DT [113-115], IN100 [116], Waspoloy [109], and HIP Astroloy [109]. The prediction of the interplay between (1) the non-crystallographic, transgranular cleavage failure mechanism near NMIs or

pores for fine grain microstructures and (2) the crystallographic crack formation failure mechanism in coarse grain microstructures becomes very important in the design of dual-microstructure Ni-base superalloy disks (e.g., [117]).

Another mesoscopic parameter that affects fatigue significantly is the distribution of grain orientation, i.e., the texture of the material. Texture development becomes especially important for highly anisotropic materials such as the HCP Ti alloys modeled in this study. For example, in duplex α/β Ti-6Al-4V alloys slip is preferred in the primary α phase via basal and prismatic slip planes since these slip planes have a lower critical resolved shear stress as compared to the primary and secondary pyramidal slip planes [78-81,118]. The fact that slip is easier on basal and prismatic planes can have major implications for rolled Titanium microstructures or clusters of grains that are preferentially oriented for basal or prismatic slip.

The minimum misorientation (i.e., disorientation) between neighboring grains plays an important role in fatigue crack formation and growth. Misorientation is the relative change in orientation between neighboring grains and can be denoted by a rotation angle/axis pair [119-120]. Grain boundaries with a high disorientation angle are often more favorable locations for fatigue crack formation [121]. This is due to the progressive pile-up of dislocations in slip bands (Zener mechanism) during cyclic loading that impinge on grain or phase boundaries, or upon oxidized inclusion interfaces, which can lead to formation and propagation of small cracks in the microstructure. Alternatively, high angle grain boundaries tend to hinder or arrest crack propagation. Specifically, the tilt and twist angles of a grain boundary directly affect the ability to transmit plasticity/slip across the grain boundary. Moreover, twin boundaries play a significant role in fcc systems [122].

Experimental techniques combining various technologies such as serial sectioning, X-ray diffraction contrast tomography, EBSD/OIM, and digital image correlation allow for very accurate characterization of microstructure statistical information including grain shape, grain size, grain orientation and grain misorientation [123-125]. Although collection of this high resolution stochastic information is crucial for more accurate reconstruction and modeling of realistic 3D microstructures, these techniques can be extremely time-consuming. This makes it experimentally infeasible to obtain this level of detail about every simlation that we run. Thus, we use the statistical information obtained from limited number of experimental characterizations as input parameters for the computational reconstruction and simulation of statistically representative 3D microstructures.

We employ two different means of polycrystalline reconstruction, a traditional Voronoi tessellation technique and a random sequential adsorption (ellipsoidal packing) algorithm. The Voronoi tessellation method is used to create microstructure instantiations with convex grain hulls. The fitting of these microstructures to a targeted grain size distribution often requires a secondary Monte Carlo or simulated annealing algorithm to optimize the grain size distribution. The use of Voronoi tessellation method has some limitations. First of all, there is a limited ability to be able to reproduce bimodal or multimodal grain size distributions 126]. In addition, the average number of neighboring cells in a random Voronoi tessellation can differ from that seen in experiments. For example, Groeber et al. [124-125] showed that the average number of neighboring cells in a fine-grained IN100 Ni-base superalloy was 12.9, which differs from that predicted (15.5) for a random Voronoi tessellation [126]. One method to overcome these drawbacks of the Voronoi tessellation method is to use a random sequential adsorption method using ellipsoids to represent grains. The approximation of grains as ellipsoids has been undertaken previously by many researchers [123-124,127-129]. In Refs. [127-128], EBSD analysis of orthogonal serial sections was used to create ellipsoidal grains and reconstruct the polycrystalline microstructure for a hot rolled pure aluminum. Similarly, Groeber et al. [123-124] used serial sectioning to characterize and reconstruct statistically representative Ni-base superalloy IN100 microstructures that incorporate distributions of grain size, grain orientation and grain misorientation. Przybyla and McDowell [129] used grain equivalent ellipsoids to more accurately model the bimodal grain distribution of a duplex Ti-6Al-4V microstructure.

4.2. Nonmetallic Inclusions (NMIs) and Pores

Inclusions and pores are introduced into powder metallurgy (PM) Ni-base superalloys during materials processing. As PM processing techniques improve, cleaner Ni-base superalloys are being developed with reduced number densities of inclusions. However, proper probabilistic modeling of PM Ni-base superalloy components should take into account the probability of occurrence of a life-limiting NMI and the effect of the inclusion on the overall probability of failure. This approach should also consider the size effects associated with testing specimen-sized versus component-sized volume domains, since the statistically weakest ``defect'' size within a volume can change with the size of the volume [130-131]. In the absence of a NMI, cracks can be initiated at pores located near the surface; Porter III et al. [132] performed load control fatigue testing on two PM supersolvus Ni-base superalloys, Rene' 88DT and IN100, with average grain sizes of 30 and 25 μm, respectively. For Rene' 88DT, cracks initiated primarily at non-metallic inclusions (NMI) near the specimen surface. For IN100, life-limiting cracks initiated from pores 70% of the time and NMI the other 30%. Also, the cracks initiated most frequently at the surface of the specimen (60%).

The size of the inclusion relative to the statistically largest grain size requires further explanation. Gabb et al. [117] investigated the fatigue mechanisms of a graded, dual-microstructure LSHR Ni-base superalloy used for a dual microstructure disk. They tested specimens from the inner ring (fine-grained), outer ring (coarse-grained), and the transition zone (contained both fine and coarse grains). They found that fine grain inner ring specimens predominantly failed due to internal NMIs that were larger than the average grain size, whereas the coarse grain outer ring and the transition zone failed from coarse grain facets. Moreover, if the inclusion is smaller than the grain size, it seems to have little effect on the amplification of driving force for fatigue crack initiation and early growth as compared to the statistically largest grain in the microstructure. On the other hand, inclusions larger than the average grain size will most likely serve as the fatigue-critical hotspots in the microstructure. Thus, the size of the largest inclusion as compared to the largest grain size, often referred to as the ALA (as large as) grain size, is a very important attribute to monitor and control during processing. This is the reason why control of inclusion (and pore) size is crucial in fine grained Ni-base superalloy microstructures which have average grain sizes ~ 3-5 μm; cracks tend to form in these fine grained microstuctures via a Stage II, non-crystallographic, transgranular cleavage-like mechanism near non-metallic inclusions (NMIs) or pores [109-111].

Another important aspect is the inclusion/matrix interface. We consider three different conditions: the inclusion is completely intact with the matrix, the inclusion is cracked, or the inclusion is partially debonded with the matrix. Previous work on martensitic gear steels showed that intact inclusions show negligible driving force for crack nucleation in the HCF regime [86]. Prasannavenkatesan et al. [86] showed that partially debonded inclusions provide the worst case condition for fatigue crack initiation and propagation, which is consistent with other investigations in a directionally solidified Ni-base superalloy [133] and a cast A356-T6 aluminum alloy [46,134]. Therefore we consider that modeling inclusions as initially partially debonded is suitable for minimum life designs. However, this interface assumption may be overly conservative depending on the loading condition, location of the inclusion (within the subsurface), and surface treatment.

4.3 Extreme Value Marked Correlation Functions

Like most damage processes, fatigue is often highly dependent on the extreme value distributions of the microstructure attributes most relevant to the operative damage mechanisms. For example, it has been shown that in ductile polycrystalline metals the processes of crack formation and propagation are dominated by the largest non-metallic inclusions [135-137] and largest grains [115, 138-139]. Moreover, multivariate extreme value distributions are likely important when multiple microstructure attributes interact to influence fatigue damage formation. For example, multiple interacting grains or grain clusters [140-143] and large textured macrozones (i.e., microtextures) [75,144-145] have been observed to influence the fatigue life in Ti alloys. The extreme value marked correlation function (EVMCF) [99,146] offers a quantitative measure to link the influence of the distributions of multiple interacting

microstructure attributes to the extreme value response based on a given applied loading condition (e.g., strain state and strain amplitude). In practice, the EVMCF is constructed by quantifying the correlated microstructure attributes that are relevant to the operant mechanism of damage formation and that are coincident with (i.e., marked by) the regions associated with the pertinent extreme value response parameters, for example the FIP in Eq. (1). These extreme value marked correlations can be compared to the unmarked correlation functions of the same type that are sampled over the entire microstructure ensemble to determine the particular correlated microstructure attributes that are most significant relative to the extreme value response. In general, this methodology can be applied to quantify the correlated microstructure attributes that are most likely to be associated with the extreme value distributions of fatigue response, providing feedback to materials development as shown in Fig. 7 and described in the following.

To define the EVMCF it is first helpful to define the probability distribution of an arbitrary extreme valued response parameter α, which can be defined as $f_{\max(\alpha)}(\alpha|\Omega)$ for a given window Ω. In words, $f_{\max(\alpha)}(\alpha|\Omega)$ describes the probability that the response parameter α is maximum for a given window (e.g., area, volume) Ω. The EVMCF then can be defined generally for n arbitrary correlated microstructure attributes $(\beta^1, \beta^2, \dots, \beta^n)$ as $F^n_{\max(\alpha)}(\beta^1, \beta^2, \dots, \beta^n|\boldsymbol{r}^1, \boldsymbol{r}^2, \dots \boldsymbol{r}^n, \Omega)$, which describes the probability that n correlated attributed $(\beta^1, \beta^2, \dots, \beta^n)$ separated by the vectors $(\boldsymbol{r}^1, \boldsymbol{r}^2, \dots \boldsymbol{r}^n)$ can be found in the same neighborhood as the extreme value response α for a given window Ω. In practice, two correlated microstructure attributes (β^1, β^2) can be described by several different standard correlation functions such as the 2-point correlation function, the radial (i.e., pair) correlation function, the lineal path correlation function, nearest neighbor correlation function, etc. Higher correlation functions can also be envisioned (e.g., 3-point) to explore correlations between more than two microstructure attributes. The type of correlation function that should be used depends on the types of microstructure relationships that are most pertinent to the operant damage mechanisms of interest. For example, the radial correlation function would not describe the anisotropy that could be described using the 2-point correlation function.

Two targeted studies were performed recently to quantify the influence of polycrystalline microstructure on fatigue of Ni-base superalloy IN100 [141] and Ti-6Al-4V [142,147] using the EVMCF. The microstructure attribute considered was the apparent Schmid factor (calculated based on the orientation of the slip plane relative to the loading direction). The response was defined in terms of the driving forces for fatigue crack formation as predicted by the Fatemi-Socie FIP in Eq. (1). Multiple SVEs were instantiated based on the microstructure statistics of experimentally characterized microstructure volumes and simulated using physics based crystal plasticity models calibrated to experiments. The SVEs were meshed and simulated using the FEM with periodic boundary conditions to simulate subsurface fatigue crack formation and in some cases traction free boundary conditions on some surfaces to simulate surface fatigue crack formation. Correlations between the apparent Schmid factors were evaluated in terms of the radial correlation function such that $R_{\max(P)}(m^g, m^{g'}|r, \Omega)dr$ is the probability that the apparent Schmid factor m^g for grain orientation g is located coincident with the extreme value FIP P in Ω and within a distance of r to $r + dr$ of the apparent Schmid factor $m^{g'}$ associated with grain orientation g' in any specified direction. Calculating the extreme value distribution of the FIPs in conjunction with the extreme value marked correlation function provides a description of the extreme value response of the microstructure as represented by the FIP P and considers the probabilities of correlated Schmid factors m^g and $m^{g'}$ (associated with the grain orientations g and g') existing in the proximity of extreme values of P in a microstructure window Ω. By comparing $R_{\max(P)}(m^g, m^{g'}|r, \Omega)dr$ with the correlation function for the same Schmid factors (i.e., grain orientation) sampled from the complete, bulk material ensemble, given by $R(m^g, m^{g'}|r, \Omega)dr$, the Schmid factors that are most probable to exist at locations of extreme value response can be identified.

Figure 8 shows the extreme value distributions of the grain scale-averaged Fatemi-Socie FIP (Eq. (1)) for three different magnitudes of the applied maximum cyclic plastic strain after three cycles for simulations of the PM Ni-base superalloy IN100 [141]. In these simulations, periodic boundary conditions were applied in all directions to simulate a bulk subsurface material condition under loading in

strain control with completely reversed strain-controlled loading (i.e., $R_\varepsilon = -1$). As can be seen in Fig. 8, in all cases the extreme value distributions of the Fatemi-Socie FIPs were well described by the Gumbel extreme value distribution (i.e., $R^2 > 0.97$). It is noted here that these results do not consider the presence of voids or non-metallic inclusions, even though it is recognized that non-metallic inclusions play a very important role in the formation of life-limiting fatigue cracks in this particular material system. However, the understanding of extreme value slip behavior is very important in contributing to the understanding of fatigue crack formation in the vicinity of inclusions/voids.

Figure 9 shows the extreme value marked radial distributions for the apparent Schmid factor associated with SVEs subjected to an applied strain amplitude of 0.005. Both octahedral $\langle 110 \rangle \{111\}$ and cube slip $\langle 110 \rangle \{100\}$ were modeled explicitly in the crystal plasticity formation and high Schmid factors for each were compared. Here we observed that grains oriented unfavorably for octahedral slip or favorably oriented for cube slip are predicted to exist with high probability at the locations of extreme value fatigue response in IN100. Moreover, clusters of grains oriented for cube slip or clusters of grains oriented for cube slip surrounded by grains oriented favorably for octahedral slip are predicted to exist with high probability at the location of the extreme value fatigue response. These simulations support the observations made in IN100 by Li et al. [116] who observed fatigue damage formation along $\{100\}$ planes in grains oriented unfavorable for octahedral slip. This also supports the hypothesis that the driving force for fatigue crack formation is highest in clusters of grains oriented for cube slip near grains oriented for octahedral slip. In the presence of non-metallic inclusions, it would therefore be expected that that clusters of grains oriented unfavorably for octahedral slip near inclusions or voids are more susceptible to fatigue crack formation than inclusions or voids that are not located in such clusters.

A similar strategy was applied to investigate the extreme value distributions of the driving forces for fatigue crack formation in four different microstructure variants of duplex Ti-6Al-4V [142] on simulations with fully periodic boundary conditions representative of subsurface or bulk material conditions. Additionally, the influence of a traction free boundary condition was also considered relative to that of fully periodic subsurface boundary conditions [147]. Multiple SVEs were simulated and loaded under strain control with an applied strain ratio of zero (i.e., $R_\varepsilon = 0$). The crystal plasticity model accounted for slip both the primary α grains and the lamellar α+β colonies. In the primary α grains that have hcp lattice structure, four different families of slip systems were explicitly considered: three $\langle 11\bar{2}0 \rangle (0001)$ basal, three $\langle 11\bar{2}0 \rangle \{10\bar{1}0\}$ prismatic, six $\langle 11\bar{2}0 \rangle \{10\bar{1}1\}$ first order pyramidal <a>, and twelve $\langle 11\bar{2}3 \rangle \{10\bar{1}1\}$ first order pyramidal <a+c> slip systems. Here, slip is modeled to be dominant in the basal and prismatic slip systems due to a relatively low critical resolved shear stress compared to the other slip systems [81]. The lamellar α+β colonies are homogenized in the model since the individual laths range in thickness from hundreds of nanometers to several microns. A crystallographic Burger's orientation relation (BOR) is maintained between the secondary α and β laths defined such that $(0001)_\alpha \,//\, \{101\}_\beta$ and $\langle 11\bar{2}0 \rangle_\alpha \,//\, \langle 111 \rangle_\beta$. The 24 possible slip systems in the lamellar region include three $\langle 11\bar{2}0 \rangle (0001)$ basal, three $\langle 11\bar{2}0 \rangle \{10\bar{1}0\}$ prismatic, six $\langle 11\bar{2}0 \rangle \{10\bar{1}1\}$ first-order pyramidal and twelve $\langle 111 \rangle \{110\}$ bcc slip systems. The bcc slip systems are transformed into the hexagonal coordinate system via the BOR. Hard slip systems in these α+β colonies are those that intersect the α-β interface. Soft deformation modes are those on which dislocations glide parallel to the α-β interface or have parallel slip planes in both the secondary α and β phases. In particular, the model used here [18] was formulated to favor single slip, which has been experimentally observed to dominate at low cyclic strain amplitudes. In addition, higher critical resolved shear stresses are required for slip in the α+β colonies to simulate these slip systems as is observed experimentally. The four microstructure variants considered in this study with varying distributions for the primary α grain and α+β colonies are defined in Table 1.

As shown in Fig. 10, the driving forces for fatigue crack formation for the microstructures with lower volume fractions of the primary α phase and smaller primary α grain sizes tended to be the lowest in magnitude for the range of microstructures considered for the simulations with the fully periodic boundary conditions. Microstructure A was also simulated with periodic boundary conditions in two orthogonal directions with traction free boundary conditions applied to two opposing faces of the cubed

shaped simulation volume in the third orthogonal direction. In this manner, the simulated volumes were representative of a thin sheet of material with a high surface to volume ratio. It can be observed in Fig. 11 that while the distributions in the driving forces for subsurface fatigue crack formation are best characterized by the extreme value Gumbel distribution, the driving forces for surface fatigue crack formation are best characterized by the extreme value Fréchet distribution. Mathematically, the extreme value Gumbel distribution describes exponential convergence of the tails of the parent (i.e., initial) distribution; the extreme value Fréchet distribution describes polynomial tails in the direction of the extreme [148]. As the exponential converges is faster than a polynomial, the extreme maxima of the Fréchet distribution are of greater magnitude than the extreme maxima of the Gumbel distribution. It logically follows that because the tails of the extreme value distributions of the driving forces for fatigue crack formation for surface-dominated cracking are best described by polynomial convergence in contrast to the extreme value driving forces for subsurface crack formation which are best described by exponential decay, the driving forces for fatigue crack formation have the potential to be highest at the surface. However, there is a large range of the extreme value distributions of the FIPs for both surface- and subsurface-dominated fatigue crack formation that overlap. This overlap in the extreme value distribution in the driving forces for crack formation perhaps explains why surface and subsurface crack formation are often both observed from experiments in the HCF and VHCF regime (cf. [145]). Additionally, when the driving forces for fatigue crack formation are highest at the surface (i.e. when the extreme value response at the surface is associated with the extreme maxima of the extreme value distribution of the FIPs), the overall fatigue lives are predicted to be shorter than when fatigue crack form subsurface where the extreme maxima of the extreme value distributions of the FIPs are of a lower magnitude.

The extreme value marked radial correlation functions for the apparent Schmid factor for Microstructure A of Ti-6Al-4V are given in Figs. 11-13 for the both correlations between the primary α grains and the α+β colonies with high Schmid factors for the various slip systems considered. Here it can be observed that primary α grains oriented favorably for basal slip have a much higher probability of being associated with the regions of extreme value driving forces for fatigue crack formation than in the overall microstructure. Additionally, hard-soft grain interactions between primary α grains oriented favorably for basal slip and primary α grains oriented favorably for pyramidal <a+c> slip or α+β colonies oriented favorably for BOR-modified bcc slip (i.e., bcc slip systems aligned with hcp systems in accordance with the Burger's orientation relationship (BOR)) correlated with increased driving forces for fatigue crack formation over the range of α+β Ti alloy systems considered. Comparing the EVMCF generated from the simulations with fully periodic boundary conditions versus those with the two surfaces with traction free boundary conditions demonstrated that the same coupled attributes likely are associated with both surface- and subsurface-dominated failure [147] even though the driving forces for the two cases are distributed differently.

The EVMCF provided a quantitative measure of the likelihood that correlated microstructure attributes can be found in the neighborhood of the extreme value response. The development of these types of statistical tools and modeling strategies are essential to describing stochastic processes in random heterogeneous materials such as fatigue crack formation in polycrystalline metals. Damage processes are particularly sensitive to the tails of distributions of the microstructure. By quantifying the correlated microstructure attributes that are the most closely associated with fatigue damage formation, better materials can be potentially be engineered by controlling these attributes, as shown schematically in Fig. 7.

5. Crack Formation and Early Growth in Notched Specimens

The previous section focused on extreme value local responses induced by microstructure heterogeneity in the absence of stress and strain field gradients. Notches in aircraft gas turbine engine components typically are of greatest concern with regard to limiting fatigue life, serving as preferential zones for fatigue crack formation and early growth. In addition to the notch, the effects of microstructure

heterogeneity on fatigue response remain and effectively are compounded by the notch root gradient field, giving rise to notch size effects that interplay with both fatigue crack formation at the grain scale and early growth out of the influence of the notch root field. Improving the prediction of variability of HCF response of notched components requires (1) an understanding of cause and effect fatigue relationships of key microstructure attributes, (2) quantification of notch size effects, (3) a means to guide process route modification to enhance fatigue resistance, and (4) experimental validation of predicted variability of fatigue life response. The work summarized here aims to address the first two items, based on recent work by Musinski and McDowell [149].

We consider a supersolvus coarse grain (CG) IN100 Ni-base superalloy with an average grain size of 34 μm and a bimodal distribution of secondary and tertiary γ' precipitates, formed during the cooling and aging processing steps after the supersolvus heat treatment. To model the complex mechanical behavior of the CG IN100 microstructure, a three-dimensional, rate-dependent, microstructure-sensitive polycrystal plasticity model described in Ref. [141] is used that captures the first order effects of grain size and the size and volume fraction of secondary and tertiary γ' precipitates. This polycrystal plasticity model was calibrated to complex cyclic stress-strain data of multiple microstructure variations at an operating temperature of 650°C with and without hold times [150] and was implemented as a user defined material (UMAT) subroutine in ABAQUS [107].

The notched components in this study were double edge-notched specimens with notch root radius ρ subjected to fully reversed tension-compression fatigue loading, with details provided in Ref. [149]. The model employed a finer mesh size of 4 μm in a localized region near the notch root (0.15ρ away from notch root) and contained a graded mesh that gradually increased to the CG size (34 μm) at the outside barrier of the polycrystal plasticity zone. The polycrystalline grain structure within the notch root region was constructed using a random sequential adsorption algorithm similar to that previously described in Refs. [123-124,129]. The values of $\mu = -0.1$ and $\sigma = 0.4$ were chosen for the target lognormal grain size (mean grain size = 34 μm) distribution function, $f(x;\mu,\sigma) = \frac{1}{x\sigma\sqrt{2\pi}}\exp\left[\frac{-(\ln(x)-\mu)^2}{2\sigma^2}\right]$, based on previous publications of fine grain IN100 grain size distributions [83,123-124, 141,151]. An example of the polycrystalline grain structure is shown in Fig. 14(a), where each grain is represented by a different color to visualize the grain structure. The cumulative Von Mises effective plastic strain within the notch root region at maximum tensile load during the third fatigue cycle is shown in Fig. 14(b). In this Figure, the values of effective plastic strain below a value of $\bar{\varepsilon}^p = 10^{-7}$ were dropped from the contour plots to display the heterogeneity of plastic slip in the microstructure. As expected, the effective plastic strain is most significant at certain grain boundaries, which results from the incompatibility of deformation between grains of different size and orientation. Plotted in Fig. 14(c) is the distribution of maximum FIP with respect to x-distance from the notch root for five different notch root sizes at strain amplitude $\varepsilon_a = \varepsilon_y$, where ε_y is the yield strain.

Since the maximum $FIP_{FS} = \Delta\Gamma_{\max}(x)$ (Eq. (1)) as a function of x-distance from the notch root is relatively linear on a log-linear plot (Fig. 14(c)), $\Delta\Gamma_{\max}(x)$ was parameterized as an exponential decay function, $\Delta\Gamma_{max}(x) = \Delta\Gamma_{max}(0)\exp\left(\frac{-\xi x}{L_d}\right)$, where ξ is a constant and L_d is the transition crack length. This log-linear best fit was used to estimate MSC growth within the notch root field, via $\frac{da}{dN} = A_{FS}\,\tau_y\,\Delta\Gamma_{max}(x)\,a$, where τ_y is the critical resolved shear stress and a is the crack length. This relation was used to construct a crack length (a_n) versus number of cycles (N) relationship, and to assess the probability of failure at any given number of cycles via the cumulative distribution function

$CDF(S_a; L_d, N) = 1 - \exp\left[-\frac{\eta\, a_n}{L_d}\right]$; here, $\eta = -\ln(0.5)$ was used to normalize the CDF so that CDF=0.5 (50% probability) when the crack extends to the transition crack length, L_d. This method of determining the CDF function is summarized in Fig. 15.

Figure 16 compares strain-life data and simulation results for smooth and notched specimens. Details of the smooth specimen computational fits to experimental data [152-154] in Ref. [149]. As seen in the Fig. 16, a notch effectively knocks the strain-life curve downward in the HCF and VHCF regimes. It is interesting to note in Fig. 16 that the polycrystal plasticity model predicts a shallow slope in the VHCF regime for smooth specimens based on calibration to experimental data in LCF and LCF-HCF transition fatigue regimes. This is a consequence of constrained microplasticity at low strain amplitudes [149].

The results for the CDF are shown in Fig. 17 for a strain amplitude of $\varepsilon_a = 0.6\varepsilon_y$. Each blue dot in Fig. 17 represents the CDF evaluated at a given number of cycles, N, for an individual instantiation of a notched specimen with a random microstructure. Therefore, since 20 different instantiations were simulated per notch root radius at this strain amplitude, there are 20 blue dots for a given x-axis value of life, N. The transition from MSC growth to LEFM-correlated long crack growth is denoted by P_f values above 0.5. The black symbols in Fig. 17 represent the mean P_f value for all 20 instantiations at a given number of cycles. As can be seen from these Figures, the benefit of using this approach is that the cumulative distribution function can be calculated for any number of cycles and any probability of failure. This approach can be applied to LCF, HCF and transition fatigue regimes to compute the total component failure. Once the crack forms to the transition length, LEFM can be used to assess crack growth to specimen failure. This framework predicts that larger notch sizes will tend to fail before smaller notch sizes, consistent with general experimental trends, in addition to microstructure size effects on crack formation and early growth within the influence of the notch root. These computationally estimated cumulative distribution functions need to be further compared with (limited) experiments for validation and further refinement.

6. Closure

Recent progress in mesoscopic modeling and simulation that employs polycrystal plasticity as the primary computational tool has been examined for applications in fatigue of Ti and Ni-base superalloys, with emphasis on the HCF and VHCF regimes which are dominated by crack formation in individual grains/phases and early growth in the neighboring microstructure. Following a brief review of the history of mesoscopic simulations that seek to quantify the role of material heterogeneity on fatigue response, a simple methodology is outlined based on fatigue indicator parameters. It is argued that the cyclic crack tip displacement serves as a useful construct as a driving force for crystallographic fatigue crack growth that bridges scales from individual grains to crack growth over larger numbers of grains based on EPFM concepts. It is shown by direct simulation of cyclic loading of stationary cracks in single crystals that the Fatemi-Socie FIP directly relates to the ΔCTD. Variability in HCF and VHCF is computationally projected by using multiple statistical volume elements and considering the extreme value distributions built up from these simulations. The concepts of marked correlation functions and are reviewed as a means to quantify the role of multiple microstructure attributes that couple to produce the extreme value FIPs in the HCF regime. An algorithm is outlined for estimating the cumulative probability distribution of cycles for crack formation and growth from notches in HCF and VHCF.

This class of approaches is promising, but much work remains to be done in terms of validation for more extensive datasets and materials, as well as extensions that consider processes of fatigue crack nucleation in more detailed and complete fashion, including the role of grain/phase boundaries, and

methods to faithfully simulate growth of microstructurally small cracks in fatigue through 3D ensembles of grains. Relatively little attention has been devoted to these issues.

Acknowledgments

C. Przybyla and D.L. McDowell would like to acknowledge the support of the NSF Center for Computational Materials Design (NSF IIP-0541678, IIP-1034968) a joint Penn State-Georgia Tech I/UCRC, in the original development of extreme value HCF and VHCF statistical methods informed by microstructure-sensitive computational models which are reviewed here. In addition, C. Przybyla is grateful for the financial support of the Air Force Research Laboratory at Wright-Patterson Air Force Base, Dayton, Ohio. Simulations were performed using the AFRL DOD Supercomputing Resource Center. W. Musinski and D.L. McDowell are grateful for the support of the Georgia Tech-Pratt & Whitney Center of Excellence. G.M. Castelluccio acknowledges the support provided by the Roberto Rocca Education Program, a graduate fellowship.

References

[1] McDowell, D.L. and Dunne, F.P.E., "Microstructure-Sensitive Computational Modeling of Fatigue Crack Formation," International Journal of Fatigue, Special Issue on Emerging Frontiers in Fatigue, Vol. 32, No. 9, 2010, pp. 1521-1542.

[2] Asaro, R.J., Micromechanics of Crystals and Polycrystals. *Advances in Applied Mechanics*, v 23, 1983, pp. 1-115.

[3] Asaro, R.J., Needleman, A. Flow localization in strain hardening crystalline solids. *Scripta metallurgica*, v 18, n 5, 1984, pp. 429-435.4

[4] McHugh, P.E., Varias, A.G., Asaro, R.J., Shih, C.F., Computational modeling of microstructures**,** *Future Generation Computer Systems*, v 5, n 2-3, 1989, pp. 295-318.

[5] Deve, H.E., Asaro, R.J., Development of plastic failure modes in crystalline materials: Shear bands in fcc polycrystals, *Metallurgical transactions. A, Physical metallurgy and materials science*, v 20 A, n 4, 1989, pp 579-593.

[6] Sham, T.L., Needleman, A., Effects of triaxial stressing on creep caviaation of grain boundaries, *Acta Metallurgica*, v 31, n 6, 1983, pp. 919-926.

[7] Christman, T., Needleman, A., Nutt, S., Suresh, S. On microstructural evolution and micromechanical modelling of deformation of a whisker-reinforced metal-matrix composite. *Materials Science & Engineering A: Structural Materials: Properties, Microstructure and Processing*, v A107, n 1-2, 1989, pp. 49-61.

[8] Needleman, A. Micromechanical modelling of interfacial decohesion. *Ultramicroscopy*, v 40, n 3, 1992, pp. 203-214.

[9] Zikry, M.A., Failure modes in cubic crystalline materials. *American Society of Mechanical Engineers, Aerospace Division (Publication) AD*, v 36, 1993, pp. 199-210.

[10] Zikry, M.A., Kao, M. Large-scale crystal plasticity computations of microstructural failure modes. *Computing Systems in Engineering: An International Journal*, v 6, n 3, 1995, p. 225.

[11] Zikry, M.A., Kao, M. Inelastic microstructural failure mechanisms in crystalline materials with high angle grain boundaries. *Journal of the Mechanics and Physics of Solids*, v 44, n 11, p 1765-1798, Nov 1996.

[12] Haddad, Y.M., Microstructural approach to the mechanical response of a class of polycrystalline systems. I. Theoretical analysis. *Res mechanica*, v 29, n 2, p 177-196, 1990

[13] Chamis, Christos C. Probabilistic composite design. *ASTM Special Technical Publication*, v 1242, 1997, pp. 23-42.

[14] Duva, J.M. Aboudi, J., Herakovich, C.T., Probabilistic micromechanics model for damaged composites. *Journal of Engineering Materials and Technology, Transactions of the ASME*, v 118, n 4, p 548-553, Oct 1996

[15] Ruggieri, C. Dodds, R.H. Numerical evaluation of probabilistic fracture parameters using WSTRESS**,** *Engineering computations*, v 15, n 1, p 49-73, 1998.

[16] Krajcinovic, D. Damage Mechanics. Elsevier, Amsterdam, 1996.

[17] Ostoja-Starzewski, M., Al-Ostaz, A., Jasiuk, I., Alzebdeh, K., Micromechanics of damage in random composites. *Probabilistic Mechanics and Structural and Geotechnical Reliability, Proceedings of the Specialty Conference*, 1996, pp. 362-363.

[18] J. Zhai and M. Zhou, "Numerical Simulation of Dynamic Crack Growth in Ceramic Composites," *Proceedings of the 12th ASCE Engineering Mechanics Conference*, pp. 1255-1258, 1998.

[19] M. Zhou and J. Zhai, Modeling of Micromechanical Fracture using a Cohesive Finite Element Method, *CP505, Shock Compression of Condensed Matter-1999,* M. D. Furnish, L. C. Chhabildas, and R. S. Hixon, eds., pp. 623-628, 1999.

[20] E. Altus, Cohesive micromechanic fatigue model. Part I. Basic mechanisms, *Mechanics of Materials*, v 11, n 4, 1991, pp. 271-280.

[21] Abdul-Latif, A. and Saanouni, K., Effect of some parameters on the plastic fatigue behavior with micromechanical approach, Internati*onal Journal of Damage Mechanics*, v 6, n 4, 1997, pp. 433-452.

[22] Nicholas, T. And Kroupa, J.L., Micromechanics analysis and life prediction of titanium matrix composites, *Journal of Composites Technology and Research*, v 20, n 2, 1998, pp. 79-88.

[23] Voyiadjis, G.Z. and Echle, R., High cycle fatigue damage evolution in uni-directional metal matrix composites using a micro-mechanical approach, *Mechanics of Materials*, v 30, n 2, 1998, pp. 91-110.

[24] Provan, J.W., Model for fatigue crack initiation in polycrystalline solids. Advances in Research on the Strength and Fracture of Materials, 4th Int. Conference on Fracture, June 19-24, 1977, Waterloo, Ontario, Pergamon Press.

[25] Provan, J.W. Fatigue reliability distribution based on probabilistic micromechanics. M*artinus Nijhoff Publ*, p 63-69, 1982.

[26] Cox, B.N. and Morris, W.L., Probabilistic model of short fatigue crack growth. Fatigue and Fracture of Engineering Materials and Structures, 10(5), 1987, pp. 419-428.

[27] Sakai, T., Tokaji, K., Ogawa, T., Probabilistic model and computer simulation on small fatigue cracks for metallic materials. Nippon Kikai Gakkai Ronbunshu, Trans. Japan Society of Mechanical Engineers, Part A, Vol. 57(539), 1991, pp. 1514-1521.

[28] K. Tanaka and **Y.** Akiniwa, Propagation and non-propagation of small fatigue cracks, in Advances in Fracture Research, Proceedings ICF7*,* Vol. 2, Houston, TX, (March 20-24 1989) 869-887.

[29] McDowell, D.L., "Basic Issues in the Mechanics of High Cycle Metal Fatigue," International Journal of Fracture, Vol. 80, 1996, pp. 103-145.

[30] Gall, K., Sehitoglu, H., Kadioglu, Y. Methodology for predicting variability in microstructurally short fatigue crack growth rates. *Journal of Engineering Materials and Technology, Transactions of the ASME*, v 119, n 2, p 171-178, Apr 1997.

[31] Hoshide, T. and Socie, D.F., Crack nucleation and growth modeling in biaxial fatigue. Engineering Fracrure Mechanics Vol. 29, No. 3, 1988, pp. 287-299.

[32] McDowell, D.L., "Damage Mechanics in Metal Fatigue: A Discriminating Perspective," International Journal of Damage Mechanics, special issue guest edited by D.L. McDowell, Vol. 8, 1999, pp. 377-403.

[33] Lacy, T.E., Talreja, R., McDowell, D.L. Effects of damage distribution on evolution. *ASTM Special Technical Publication*, v 1315, p 131-149, Oct 1997.

[34] T. Kanit, S. Forest, L. Galliet, V. Mounoury, D. Jeulin, Int. J. Solids Struct. 40 (13–14) (2003) 3647–3679.

[35] S. R. Niezgoda, D. M. Turner, D. T. Fullwood, S. R. Kalidindi, Optimized Structure Based Representative Volume Element Sets Reflecting the Ensemble Averaged 2-Point Statistics, Acta Materialia, 58(2010) 4432–4445.

[36] D. L. McDowell, S. Ghosh, S. R. Kalidindi, Representation and Computational Structure-Property Relations of Random Media, JOM, 63(2011) 45-51.

[37] Bennett, V.P., "A Microscale Study of Small Crack Propagation in Multiaxial Fatigue," PhD thesis, Georgia Tech, 1999.

[38] Bennett, V. and McDowell, D.L., "Polycrystal Orientation Effects on Microslip and Mixed Mode Behavior of Microstructurally Small Cracks," Mixed-Mode Crack Behavior, ASTM STP 1359, Eds. K.J. Miller and D.L. McDowell, 1999, pp. 203-228.

[39] Bennett, V.P. and McDowell, D.L., "Crystal Plasticity Analyses of Stationary, Microstructurally Small Surface Cracks in Ductile Single Phase Polycrystals," Fatigue and Fracture of Engineering Materials and Structures, Vol. 25, No. 7, 2002, pp. 677-693.

[40] Bennett, V.P. and McDowell, D.L., "Crack Tip Displacements of Microstructurally Small Surface Cracks in Single Phase Ductile Polycrystals," Engineering Fracture Mechanics, Vol. 70, 2003, pp. 185-207.

[41] Bennett, V.P. and McDowell, D.L., "Polycrystal Orientation Distribution Effects on Microslip in High Cycle Fatigue," International Journal of Fatigue, Vol. 25, 2003, pp. 27-39.
[42] Gall, K., Yang, N., Horstemeyer, M., McDowell, D.L., and Fan, J.,"The Debonding and Fracture of Si Particles During the Fatigue of a Cast Al-Si Alloy," Metallurgical and Materials Transactions A, Vol. 30A, 1999, pp. 3079-3088.
[43] Gall, K., Horstemeyer, M., McDowell, D.L., and Fan, J. "Finite Element Analysis of the Stress Distributions Near Damaged Si Particle Clusters in Cast Al-Si Alloys," Mechanics of Materials, Vol. 32, No. 5, 2000, pp. 277-301.
[44] Gall, K., Horstemeyer, M.F, Degner, B.W., McDowell, D.L., and Fan, J. "On the Driving Force for Fatigue Crack Formation From Inclusions and Voids in a Cast A356 Aluminum Alloy," International Journal of Fracture, Vol. 108, 2001, pp. 207-2
[45] Fan, J., McDowell, D.L., Horstemeyer, M.F. and Gall, K., "Computational Micromechanics Analysis of Cyclic Crack-tip Behavior for Microstructurally Small Cracks in Dual-Phase Al-Si Alloys", Engineering Fracture Mechanics, Vol. 68, 2001, pp. 1687-1706.
[46] McDowell, D.L., Gall, K., Horstemeyer, M.F. and Fan, J., "Microstructure-Based Fatigue Modeling of Cast A356-T6 Alloy," Engineering Fracture Mechanics, Vol. 70, 2003, pp. 49-80.
[47] Tryon, R.G., Cruse, T.A., Reliability-based mesomechanical crack nucleation model. Collection of Technical Papers – AIAA/ASME/ASCE/AHS/ASC Structures, Structural Dynamics and Materials Conference, Vol. 4, 1996, pp. 2159-2166.
[48] Tryon, R.G., Cruse, T.A., Probabilistic mesomechanics for high cycle fatigue life prediction. ASME Journal of Engineering Materials and Technology, Vol. 119(1), 1997a, pp. 65-70.
[49] Tryon, R.G. and Cruse, T.A., Probabilistic mesomechanics for high cycle fatigue life prediction. ASME Aerospace Division Publication AD, Vol. 55, 1997b, pp. 467-474.
[50] Manonukul A, Dunne FPE. High and low cycle fatigue crack initiation using polycrystal plasticity. Proc. R. Soc. Lond. 2004;460, 2047:1881-1903.
[51] Dunne FPE, Rugg D, Walker A. A systematic study of hcp crystal orientation and morphology effects in polycrystal deformation and fatigue. Proc. R. Soc. London 2007;463, 2082:1467-1489.
[52] Dunne FPE, Walker A, Rugg D. Lengthscale-dependent, elastically anisotropic, physically-based HCP crystal plasticity: application to cold-dwell fatigue in Ti alloys. Intl. Journal of Plasticity 2007;23:1061-1083.
[53] Saheli G, Garmestani H, Gokhale A. Homogenization [125] Dunne FPE, Wilkinson A, Allen R. Experimental and computational studies of low cycle fatigue crack nucleation in a polycrystal. Int. J. Plasticity 2007;23(2):273-295.
[54] Korsunsky AM, Dini D, Dunne FPE, and Walsh, MJ. Comparative assessment of dissipated energy and other fatigue criteria. Int. J. Fatigue 2007:29(9-11):1990-1995.
[55] Dunne FPE, Rugg D. On the mechanisms of fatigue facet nucleation in titanium alloys. Fatigue and Fract. Engng. Mater. Structures 2008;31:949-958.
[56] Venkataramani G, Deka D, Ghosh S, Nordholt JB. Crystal plasticity based Fe model for understanding microstructural effects on creep and dwell fatigue in Ti-6242. Journal of Engineering Materials and Technology, Transactions of the ASME 2006;128(3):356-365.
[57] Manchiraju S, Kirane K, Ghosh S. Dual-time scale crystal plasticity FE model for cyclic deformation of Ti alloys. Journal of Computer-Aided Materials Design 2007;14(1):47-61.
[58] Kirane K, Ghosh S. A cold dwell fatigue crack nucleation criterion for polycrystalline Ti-6242 using grain-level crystal plasticity FE Model. International Journal of Fatigue 2008;30(12):2127-2139.
[59] Kirane, K., Ghosh, S., Groeber, M., and Bhattacharjee, A. (2009) "Grain level dwell fatigue crack nucleation model for ti alloys using crystal plasticity finite element analysis," *Journal of Engineering Materials and Technology* 131(2):021003 1–14.

[60] McDowell, D.L. (2005) "Microstructure-sensitive computational fatigue analysis," Handbook of Materials Modeling, Part A: Methods, eds. Sidney Yip and M.F. Horstemeyer, Springer, the Netherlands, pp.1193-1214.
[61] McDowell, D.L. (2007) "Simulation-based strategies for microstructure-sensitive fatigue modeling," *Materials Science and Engineering* A, Vol. 468-470, 2007, Pages 4-14.
[62] McDowell, D.L., "Microstructure-Sensitive Modeling and Simulation of Fatigue," *ASM Handbook* on *Fundamentals of Modeling for Metals Processing*, Handbook Vol. 22A, ASM International, 2009, ISBN 13:978-1-61503-001-0.
[63] McDowell, D.L. (1996) "Multiaxial fatigue strength," *ASM Handbook*, Vol. 19 on Fatigue and Fracture, ASM International, pp. 263-273.
[64] McDowell, D.L. and Bennett, V. (1997) "Micromechanical aspects of small multiaxial fatigue cracks," Proc. 5th Int. Conf. On Biaxial/Multiaxial Fatigue & Fracture, Cracow, Poland, pp. 325-348.
[65] Apelian, D. (2004) ch. National Research Council Report, *Accelerating Technology Transition,* National Academies Press, Washington DC.
[66] Whitis, D. and Schafrik, R., (2007) "Materials modeling and simulation—a game changing technology for propulsion materials development," ASM/TMS Symposium - Computational Materials Design, Niskayuna, NY, Aug. 20-22.
[67] McDowell, D.L. and Backman, D., "Simulation-Assisted Design and Accelerated Insertion of Materials," Ch. 19 in *Computational Methods for Microstructure-Property Relationships*, Eds. S. Ghosh and D. Dimiduk, Springer, 2010, ISBN 978-1-4419-0642-7.
[68] McDowell, D.L. and Olson, G.B., "Concurrent Design of Hierarchical Materials and Structures," *Scientific Modeling and Simulation* (CMNS), Vol. 15, No. 1, 2008, p. 207.-240.
[69] Larsen, J. and Christodoulou, L. (2004) "Integrating damage state awareness and mechanism-based prediction," JOM, Vol. 56, No. 3, p. 14.
[70] Larsen, J., John, R. and Lindgren, E. (2008) 'Opportunities and challenges in damage prognosis for materials and structures in complex systems ," AFOSR Discovery Challenge Thrust (DCT) Workshop on Prognosis of Aircraft and Space Devices, Components, and Systems, Cincinnati, OH, Feb. 18-20.
[71] Fatemi A. and Socie, D.F. (1988) "Critical plane approach to multiaxial fatigue damage including out-of-phase loading," *Fat Fract Engng Mater Struct.,* Vol. 11, No. 3, pp. 149–65.
[72] Fatemi, A. and Kurath, P. (1988) "Multiaxial fatigue life predictions under the influence of mean-stresses," *ASME Journal of Engineering Materials Technology*, Vol. 110, pp. 380–388.
[73] Socie, D. F. (1993) "Critical plane approaches for multiaxial fatigue damage assessment," in *Advances in Multiaxial Fatigue*, eds D.L. McDowell and R. Ellis. ASTM STP 1191, ASTM, Philadelphia, pp. 7–36.
[74] Vehoff, H., Nykyforchyn, A., and Metz, R. (2004) Fatigue crack nucleation at interfaces. Materials Science and Engineering A 387-389(1-2):546-551.
[75] Le Biavant K, Pommier S, Prioul C. Local texture and fatigue initiation in a Ti-6Al-4V titanium alloy. Fatigue Fract Eng Mater Struct 2002;25:527–45.
[76] Morrison DJ, Moosbrugger JC. Effects of grain size on cyclic plasticity and fatigue crack initiation in nickel. Int J Fatigue 1997;19:S51–9.
[77] McDowell, D.L., "Viscoplasticity of Heterogeneous Metallic Materials," Materials Science and Engineering R: Reports, Vol. 62, Issue 3, 2008, pp. 67-123.
[78] Mayeur, J.R. and McDowell, D.L., "A three-dimensional crystal plasticity model for duplex Ti-6Al-4V," *Int. J. of Plasticity*, Vol. 23, No. 9, 2007, pp. 1457-1485.
[79] Zhang, M., Zhang, J. and McDowell, D.L. (2007) "Microstructure-based crystal plasticity modeling of cyclic deformation of Ti-6Al-4V," *Int. J. of Plasticity*, Vol. 23, No. 8, pp. 1328-1348.

[80] Bridier, F., Villechaise, P., Mendez, J. (2007) "Analysis of slip and crack initiation processes activated by fatigue in a □□□ titanium alloy in relation with local crystallographic orientation," Fatigue 2006, May 2006, Atlanta, GA.

[81] Bridier, F., McDowell, D.L., Patrick Villechaise, P., and Mendez, J., "Crystal Plasticity Modeling of Slip Activity in Ti-6Al-4V under High Cycle Fatigue Loading," International Journal of Plasticity, Vol. 25, No. 6, 2009, pp. 1066-1082.

[82] Kumar, R.S., Wang, A.-J., and McDowell, D.L. (2006) "Effects of microstructure variability on intrinsic fatigue resistance of nickel-base superalloys – a computational micromechanics approach," *Int. J. Fract*., Vol. 137, pp. 173 - 210.

[83] Shenoy, M., Zhang, J., and McDowell, D.L. (2007) "Estimating fatigue sensitivity to polycrystalline Ni-base superalloy microstructures using a computational approach," *Fatigue and Fract. Eng. Mat. Struct.*, Vol. 30, No. 10, pp.889-904.

[84] Zhang, J., Prasannavenkatesan, R., Shenoy, M.M., and McDowell, D.L., "Modeling Fatigue Crack Nucleation at Primary Inclusions in Carburized and Shot-Peened Martensitic Steel," *Engineering Fracture Mechanics*, Vol. 76, No. 3, 2009, pp. 315-334.

[85] Prasannavenkatesan, R., Zhang, J., McDowell, D.L., Olson, G.B., and Jou, H.-J., "3D Modeling of Subsurface Fatigue Crack Nucleation Potency of Primary Inclusions in Heat Treated and Shot Peened Martensitic Gear Steels," International Journal of Fatigue, Vol. 31, No. 7, 2009, pp. 1176-1189.

[86] Prasannavenkatesan, R. McDowell, D.L., Olson, G.B., and Jou, H.-J., "Modeling Effects of Compliant Coatings on HCF Resistance of Primary Inclusions in High Strength Steels," ASME Journal of Engineering Materials and Technology, Vol. 131, 2009, pp. 0110112-1-6.

[87] T. Hoshide and D. Socie, Mechanics of mixed mode small fatigue crack growth, E*ngineering Fracture Mechanics* 26(6) (1987) 842-850.

[88] D. L. McDowell and J. Y. Berard. A ΔJ-based approach to biaxial fatigue. Fatigue and Fracture of Engineering Materials and Structures, 15(8):719-741, 1992.

[89] H. Mughrabi, "On 'multi-stage' fatigue life diagrams and the relevant life-controlling mechanisms in ultrahigh-cycle fatigue," *Fatigue & Fracture of Engineering Materials & Structures* 25, no. 8-9 (2002): 755-764.

[90] Sangid MD, Maier HJ, Sehitoglu H, "A physically-based model for prediction of crack initiation from persistent slip bands in polycrystals," *Acta Materialia* 59 328-341 (2011).

[91] Sangid, M., H. Sehitoglu, H.J. Maier, An energy-based microstructure model to account for fatigue scatter in polycrystals", J. Mechanics and Physics of Solids, 59, 3,595-609, 2011.

[92] Tanaka K, and Mura T. A dislocation model for fatigue crack initiation. ASME J. Appl. Mech. 1981;48(1):97–103.

[93] Venkataraman G, Chung YW, Mura T. Application of minimum energy formalism in a multiple slip band model for fatigue - II. Crack nucleation and derivation of a generalized Coffin-Manson law. Acta Metall. Mater. 1991;39:2631-2638.

[94] U. Essmann, U. Gosele, and H. Mughrabi. A model of extrusions and intrusions in fatigued metals .1. Point-Defect production and the growth of extrusions. *Philosophical Magazine a-Physics of Condensed Matter Structure Defects and Mechanical Properties*, 44(2):405–426, 1981.

[95] Polak, J., On the role of point defects in fatigue crack initiation, Materials Science and Engineering, 92, 1987, pp. 71-80.

[96] Polak, J. And Sauzay, M., "Growth of extrusions in localized cyclic plastic straining," Materials Science and Engineering A 500 (2009):122-129.

[97] W. Egger, G. Kogel, P. Sperra, W. Triftshauser, S. Rodling, J. Bar, H.-J. Gudladt, "Vacancy clusters close to a fatigue crack observed with the Munchen scanning positron microscope," Applied Surface Science 194 (2002) 214–217.

[98] W. Egger a,∗, G. Kögel a, P. Sperr a, W. Triftshäuser a, J. Bärb, S. Rödling b, H.-J. Gudladt, Measurements of defect structures of a cyclically deformed Al–Mg–Si alloy by positron annihilation techniquesMat. Sci Eng. A 387-389 (2004): 317-320.

[99] C. P. Przybyla, "Microstructure-sensitive Extreme Value Probabilities of Fatigue in Advanced Engineering Alloys," in *Materials Science and Engineering*. vol. Doctor of Philosophy Atlanta: Georgia Institute of Technology, 2010, pp. 1-328.

[100] D. F. Socie and G. B. Marquis. Multiaxial Fatigue. SAE International, 1999.

[101] S.C. Reddy, A. Fatemi, M. R. Mitchell, and R. W. Landgraf. Small crack growth in multiaxial fatigue. In Advances in Fatigue Lifetime Predictive Techniques, STP 1122, 276-298. ASTM, 1992.

[102] Shih, C.F., "Relationsihps Between the J-Integral and Crack Opening Displacement for Stationary and Extending Cracks," Journal of the Mechanics and Physics of Solids, Vol. 29(4), 1981, pp. 305-326.

[103] Brown, M. and Miller, K.J., "A Theory for Fatigue Failure under Multiaxial Stress-Strain Conditions," Proc. Inst. Mech. Engrs., Vol. 187, No. 65, 1973, pp. 745-755.

[104] D. Hellmann and K. H. Schwalbe. Geometry and size effects on J-R and δ-R curves under plane stress conditions. In Fracture mechanics: fifteenth symposium, STP 833, 577-603. ASTM, 1984.

[105] Castelluccio, G.M. and McDowell, D.L., "Effect of a deformation band on crack tip displacement simulations under cyclic loading," 5th International Conference on Very High Cycle Fatigue, Berlin, Germany, June 28-30, 2011.

[106] G. M. Castelluccio and D. L. McDowell. Assessment of Small Fatigue Crack Growth Driving Forces in Single Crystals with and without Slip Bands, submited to Int. J. Fatigue, 2011 (in review

[107] ABAQUS. FEM software v6.9, Simulia Inc., Providence RI, USA, 2009.

[108] F. Ma, X. Deng, M. A. Sutton, J. C. Newman, K. Miller, and D. L. McDowell. A CTOD-based mixed-mode fracture criterion. In Mixed-Mode Crack Behavior, STP 1359, pages 86{110. ASTM, 1999.

[109] Gayda, J., Miner, R.V., 1983. Fatigue crack initiation and propagation in several nickel-base superalloys at 650°C. Int. J. Fatigue, 5(3):135-143.

[110] Caton, M., Jha, S., 2010. Small fatigue crack growth and failure mode transitions in a Ni-base superalloy at elevated temperature. Int. J. Fatigue, 32:1461-1472.

[111] Pang, H., and Reed, P., 2007. Microstructure effects on high temperature fatigue crack initiation and short crack growth in turbine disc nickel-base superalloy udimet 720Li. Mater. Sci. Eng., A, 448(1-2):67-79.

[112] Pineau, A., Antolovich, S.D., 2009. High temperature fatigue of nickel-base superalloys - a review with special emphasis on deformation modes and oxidation. Engineering Failure Analysis, 16(8):2668-2697.

[112] Stöcker, C., Zimmermann, M., Christ, H., 2011. Localized cyclic deformation and corresponding dislocation arrangements of polycrystalline Ni-base superalloys and pure nickel in the VHCF regime. Int. J. Fatigue, 33:2-9.

[113] Shyam, A., Torbet, C., Jha, S., Larsen, J., Caton, M., Szczepanski, C., Pollock, T., Jones, J., 2004. Development of ultrasonic fatigue for rapid, high temperature fatigue studies in turbine engine materials. In Superalloys 2004, 259-268, The Minerals, Metals and Materials Society.

[114] Jha, S.K., Caton, M.J., Rosenberger, A.H., Li, K., Porter, W.J., 2005. Super-imposing mechanisms and their effect on the variability in fatigue lives of a nickel-based superalloy. In Materials Damage Prognosis, 343-350, TMS.

[115] Miao, J., Pollock, T.M., Jones, J.W., 2009. Crystallographic fatigue crack initiation in nickel-based superalloy Rene 88DT at elevated temperature. Acta Mater., 57(20):5964-5974.

[116] Li, K., Ashbaugh, N., Rosenberger, A., 2004. Crystallographic initiation of nickel-base superalloy IN10 at RT and 538°C under low cycle fatigue conditions. In Superalloys 2004,TMS, Champion, PA, 251-258..

[117] Gabb, T.P., Kantzos, P.T., Telesman, J., Gayda, J., Sudbrack, C.K., Palsa, B., 2011. Fatigue resistance of the grain size transition zone in a dual microstructure superalloy disk. Int J Fatigue, 33:414-426.

[118] Zhang, M., Bridier, F., Villechaise, P., Mendez, J., and McDowell, D.L., "Simulation of Slip Band Evolution in Duplex Ti-6Al-4V," Acta Materialia, Vol.. 58, 2010, pp. 1087-1096.

[119] Randle, V., 1993. The measurement of grain boundary geometry. In Electron Microscopy in Materials Science Series. Institute of Physics Publishing, Bristol, UK.

[120] Engler, O., Randle, V., 2010. Introduction to Texture Analysis: macrotexture, microtexture, and orientation mapping. CRC Press, Taylor & Francis Group, Boca Raton, FL.

[121] Birosca, S., Buffiere, J.Y., Garcia-Pastor, F.A., Karadge, M., Babout, L., Preuss, M., 2009. Three-dimensional characterization of fatigue cracks in Ti-6246 using X-ray tomography and electron backscatter diffraction. Acta Mater, 57:5834-5847.

[122] Sangid, M.D., Maier, H.J., and Sehitoglu, H., "The role of grain boundaries on fatigue crack initiation – An energy approach," International Jourhal of Plasticity, 27(5) *2011:801-821.*

[123] Groeber, M., Ghosh, S., Uchic, M.D., Dimiduk, D.M., 2008a. A framework for automated analysis and simulation of 3D polycrystalline microstructures.: Part 1: Statistical characterization. Acta Mater., 56(6):1257-1273.

[124] Groeber, M., Ghosh, S., Uchic, M.D., Dimiduk, D.M., 2008b. A framework for automated analysis and simulation of 3D polycrystalline microstructures. part 2: Synthetic structure generation. Acta Mater., 56(6):1274-1287.

[125] Herbig, M., King, A., Reischig, P., Proudhon, H., Lauridsen, E.M., Marrow, J., Buffiere, J.-Y., Ludwig, W., 2011. 3-D growth of a short fatigue crack within a polycrystalline microstructure studied using combined diffraction and phase-contrast X-ray tomography. Acta Mater, 59:590-601.

[126] Xu, T., Li, M., 2009. Topological and statistical properties of a constrained Voronoi tessellation. Philos Mag, 89(4):349-374.

[127] Saylor, D.M., Fridy, J., El-Dasher, B.S., Jung, K.-Y., Rollett, A.D., 2004. Statistically representative three-dimensional microstructures based on orthogonal observation section. Metall Mater Trans A, 35A:1969-1979.

[128] Brahme, A., Alvi, M.H., Saylor, D., Fridy, J., Rollett, A.D., 2006. 3D reconstruction of microstructure in a commercial purity aluminum. Scripta Mater, 55:75-80.

[129] Przybyla, C.P., McDowell, D.L., 2010. Simulation-based extreme value marked correlations in fatigue of advanced engineering alloys. Procedia Engineering, 2(1):1045-1056.

[130] Pineau, A., 1990. Superalloy discs durability and damage tolerance in relation to inclusions. Proceedings of a Conference on High Temperature Materials for Power Engineering 1990, 913-934.

[131] Reed, R.C., 2006. The Superalloys; Fundamentals and Applications. Cambridge University Press, Cambridge, UK.

[132] Porter III, W., Li, K., Caton, M., Jha, S., Bartha, B., Larsen, J., 2008. Microstructural conditions contributing to fatigue variability in P/M nickel-base superalloys. In 11th International Symposium on Superalloys, Superalloys 2008, September 14, 2008 - September 18, 2008, Proceedings of the International Symposium on Superalloys, 541-548. Champion, PA: The Minerals, Metals and Materials Society.

[133] Shenoy, M.M., Kumar, R.S., McDowell, D.L., 2005. Modeling effects of nonmetallic inclusions on LCF in DS nickel-base superalloys. Int J Fatigue, 27:113-127.

[134] Fan, J., McDowell, D.L., Horstemeyer, M.F., Gall, K., 2003. Cyclic plasticity at pores and inclusions in cast Al-Si alloys. Eng Fract Mech, 70:1281-1302.

[135] Y. Murakami, S. Kodama, and S. Konuma, "Quantitative evaluation of defects of non-metallic inclusions on fatigue strength of high strength steels. I: Basic fatigue mechanism and evaluation of correlation between the fatigue fracture stress and the size and location of non-metallic inclusions.," *International Journal of Fatigue,* vol. 11, pp. 291-298, Sep 1989.

[136] Y. Murakami and H. Usuki, "Quantitative evaluation of effects of non-metallic inclusions on fatigue strength of high strength steels. II: Fatigue limit evaluation based on statistics for extreme values of inclusion size," *International Journal of Fatigue,* vol. 11, pp. 299-307, 1989.

[137] Prasannavenkatesan, R., Pryzbyla, C.P., Salajegheh, N., and McDowell, D.L. ”Simulated Extreme Value Fatigue Sensitivity to Inclusions and Pores in Martensitic Gear Steels,” Engineering Fracture Mechanics, Vol. 78, No. 6, 2011, pp. 1140-1155.

[138] Y. S. Choi and T. A. Parthasarathy, "A crystal-plasticity finite element method study on effect of abnormally large grain on mesoscopic plasticity of polycrystal," *Scripta Materialia,* vol. 66, 2012, pp. 56-59.

[139] M. L. Brogdon and A. H. Rosenberger, "Evaluation of the Influence of Grain Structure on the Fatigue Variability of Waspaloy," in *Superalloys*, R. C. Reed, K. A. Green, P. Caron, T. P. Gabb, M. G. Fahrmann, E. S. Juron, and S. A. Woods, Eds.: TMS (The Minerals, Metals & Materials Society), 2008, pp. 583-588.

[140] Y. Guilhem, S. Basseville, F. Curtit, J. M. Stéphan, and G. Cailletaud, "Investigation of the effect of grain clusters on fatigue crack initiation in polycrystals," *International Journal of Fatigue,* vol. 32, pp. 1748-1763.

[141] C. P. Przybyla and D. L. McDowell, "Microstructure-sensitive extreme value probabilities for high cycle fatigue of Ni-base superalloy IN100," *International Journal of Plasticity,* vol. 26, 2010, pp. 372-394.

[142] C. P. Przybyla and D. L. McDowell, "Microstructure-Sensitive Extreme Value Probabilities for High Cycle Fatigue of Ti-6Al-4V," *International Journal of Plasticity,* vol. 27, pp. 1871-1895, 2011.

[143] J. L. Gilbert and H. R. Piehler, "On the nature and crystallographic orientation of subsurface cracks in high cycle fatigue of Ti-6Al-4V," *Metallurgical Transactions A,* vol. 24, pp. 669-680, 1993.

[144] F. Bridier, P. Villechaise, and J. Mendez, "Slip and fatigue crack formation processes in an a/b titanium alloy in relation to crystallographic texture on different scales," *Acta Materialia,* vol. 56, pp. 3951-3962, 2008.

[145] C. J. Szczepanski, S. K. Jha, J. M. Larsen, and J. W. Jones, "Microstructural influences on very-high-cycle fatigue-crack initiation in Ti-6246," *Metallurgical and Materials Transactions A,* vol. 39A, 2008, pp. 2841-2851.

[146] C. Przybyla, R. Prasannavenkatesan, N. Salajegheh, and D. L. McDowell, "Microstructure-sensitive modeling of high cycle fatigue," *International Journal of Fatigue,* vol. 32, pp. 512-525, 2009.

[147] C. P. Przybyla and D. L. McDowell, "Microstructure-sensitive extreme-value probabilities of high-cycle fatigue for surface vs. subsurface crack formation in duplex Ti-6Al-4V," *Acta Materialia,* vol. 60, pp. 293-305, 2012.

[148] A. Haldar and S. Mahadevan, *Probability, Reliability and Statistical Methods in Engineering Design*. New York: John Wiley & Sons, Inc., 2000.

[149] Musinski, W.D., McDowell, D.L., 2012. Microstructure-sensitive probabilistic modeling of HCF crack initiation and early crack growth in Ni-base superalloy IN100 notched components. International Journal of Fatigue, 37:41-53.

[150] Shenoy, M., Tjiptowidjojo, Y., McDowell, D.L., 2008. Microstructure-sensitive modeling of polycrystalline IN100. Int. J. Plasticity, 24(10):1694-1730.

[151] Wusatowska-Sarnek, A.M., Ghosh, G., Olson, G.B., Blackburn, M.J., Aindow, M., 2003. Characterization of the microstructure and phase equilibria calculations for the powder metallurgy superalloy IN100. J. Mater. Res., 18(11):2653-2663.

[152] Cowles, B.A., Sims, D.L., Warren, J.R., 1978. Evaluation of the cyclic behavior of aircraft turbine disk alloys. NASA CR-159409.

[153] Cowles, B.A., Warren, J.R., Haake, F.K., 1980. Evaluation of the cyclic behavior of aircraft turbine disk alloys, Part II. NASA CR-165123.

[154] Bathias, C., Paris, P.C., 2010. Gigacycle fatigue of metallic aircraft components. Int. J. Fatigue, 32(6):894-897.

Tables

Table 1. Microstructures for Ti-6Al-4V along with the assumed log-normal fits for the grain volume distributions.

		Duplex Ti-6Al-4V Microstructures			Assumed Mean and St. Dev. for Grain Size Distributions			
					α+β Colony		Primary α	
Micro.	Type	Transformed β Size (μm)	Primary α Size (μm)	Vol % Primary α	μ (μm)	σ (μm)	μ (μm)	σ (μm)
A	Fine bi-modal low α	50	10-50	30%	50	5	25	10
B	Fine bi-modal high α	50	10-50	70%	50	5	25	10
C	Coarse bi-modal low α	80	40-60	30%	80	10	50	5
D	Coarse bi-modal high α	80	40-60	70%	80	10	50	5

Figures

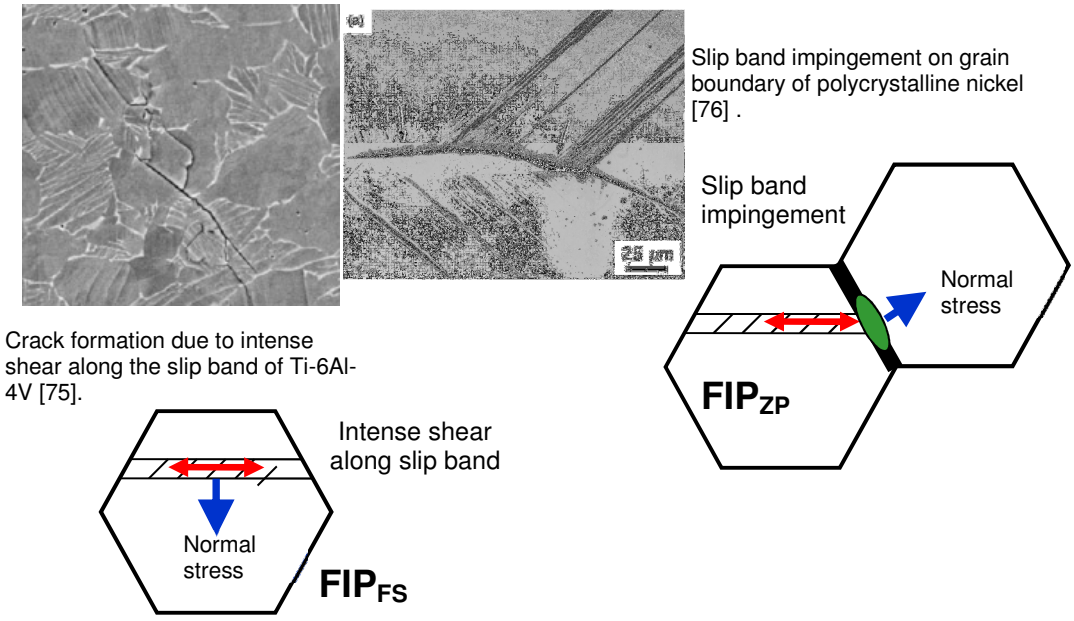

Fig. 1. Candidate fatigue indicator parameters (FIPs) with combined plastic shear strain and normal stress effects on candidate planes for crack nucleation and early growth along slip bands or grain boundaries for Ti-6Al [75] and Ni [76].

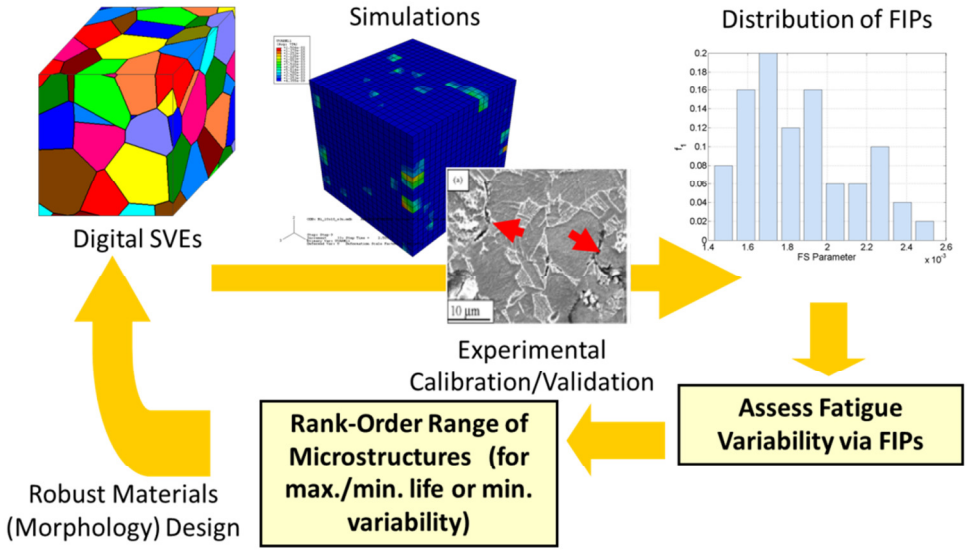

Fig. 2. Overall concept of using simulations from multiple SVEs instantiated using spatial statistics of representative microstructures to compute the distribution of FIPs and estimate the variability of fatigue response, using this information to rank order microstructures and to provide feedback to process route and structure to improve material performance [99].

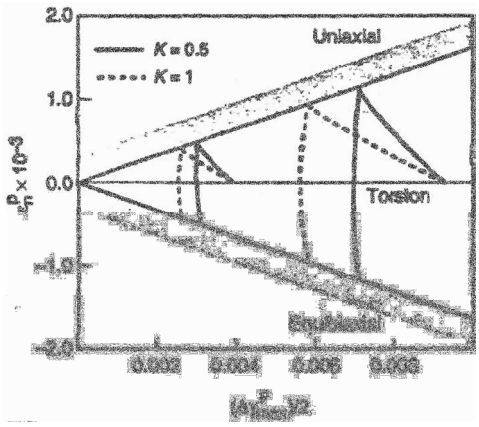

Fig. 3. Constant life contour plots in Γ^p -plane (based on plastic strain) for two different LCF lives based on the Fatemi-Socie parameter (reproduced from Ref. [63]).

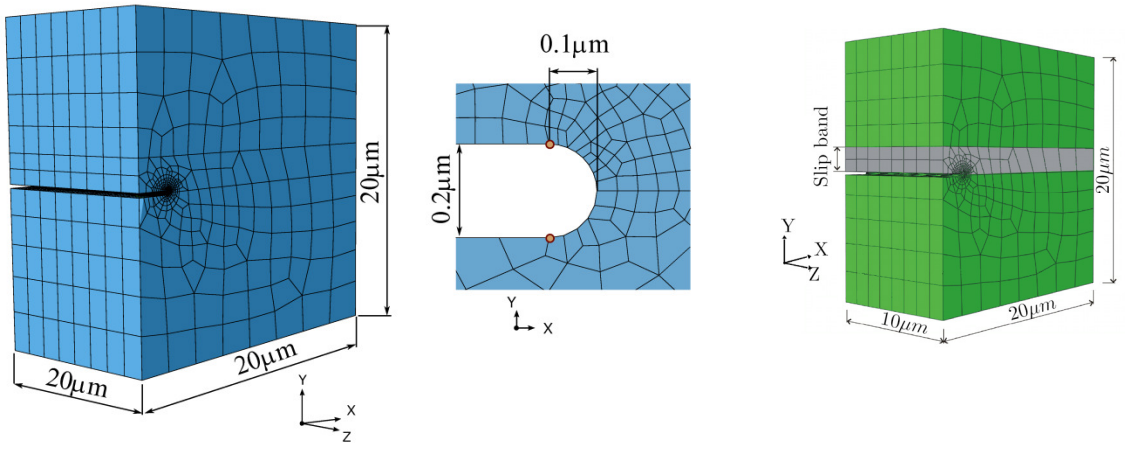

Fig. 4. Cracked single crystal employed to evaluate the fine scale FIP and ΔCTD measured between nodes in red at the mid-thickness for cyclically loaded stationary cracks. The crystallographic planes are oriented so that the crack plane is an octahedral slip plane with a slip direction along the X-axis.

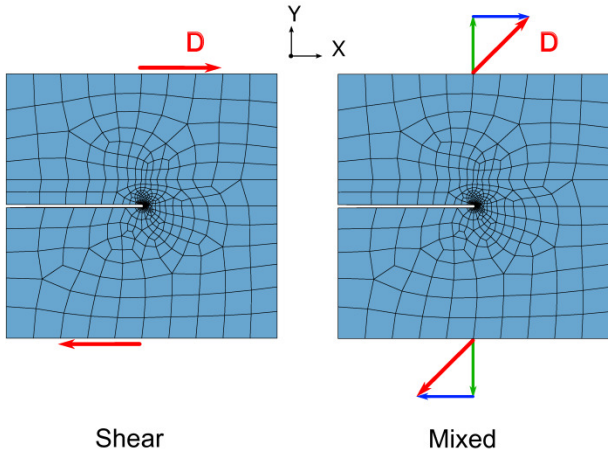

Fig. 5. Shear (left) and mixed mode (right) loading cases employing the same magnitude of the displacement vector (**D**).

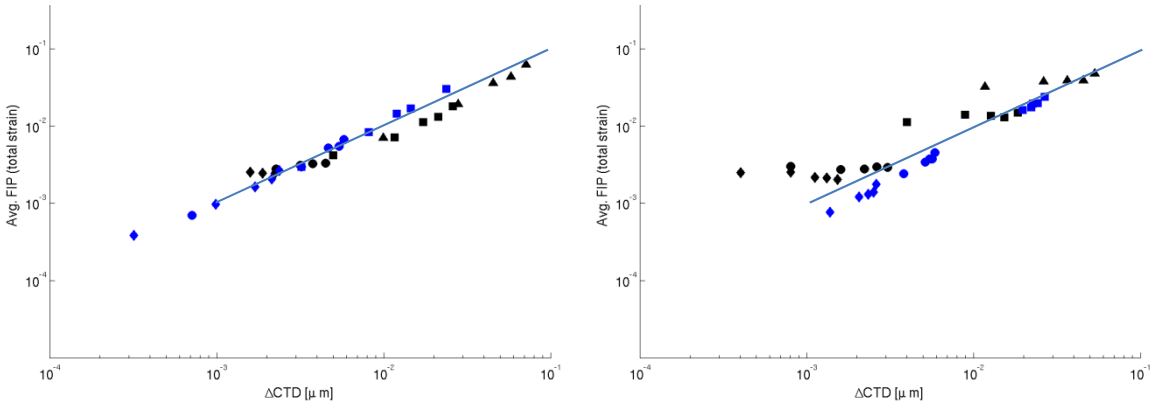

Fig. 6. Comparison of computed fine scale FIP versus ΔCTD for (left) shear and (right) mixed mode loading for Cu (blue symbols) and RR1000 Ni-base superalloy (black symbols) with small cracks under cyclic loading; solid lines have unity slope, indicating a linear relation.

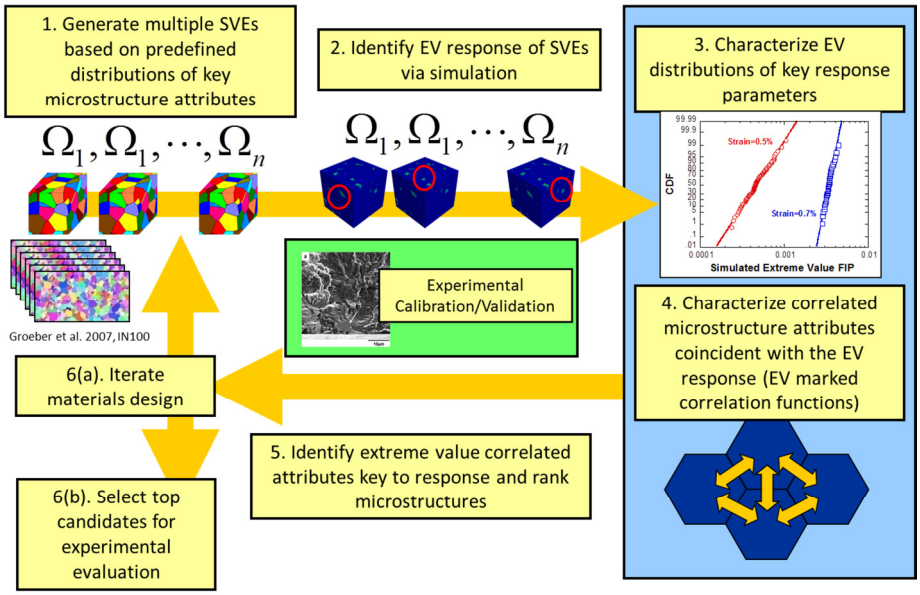

Fig. 7. Schematic of a microstructure-sensitive probabilistic framework of extreme value type in which simulations of many SVE instantiations provides feedback to processing and materials develop microstructures with improved performance/variability in HCF [99].

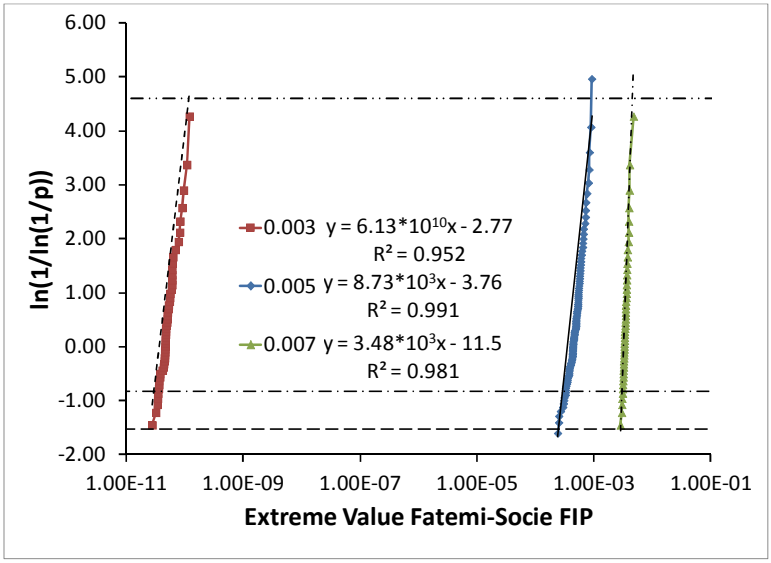

Fig. 8. For IN100, the grain averaged extreme value Fatemi-Socie (FS) FIP for the SVEs cycled at 0.3%, 0.5%, and 0.7% maximum strain are plotted on Gumbel probability scales. Note that the equations given for the least squares linear regression are such that $y = \ln\left(1/\ln(1/p)\right)$ and $x = extreme\ value$ FIP. The extreme value FIP for each SVE was selected to as the maximum of those calculated over each grain.

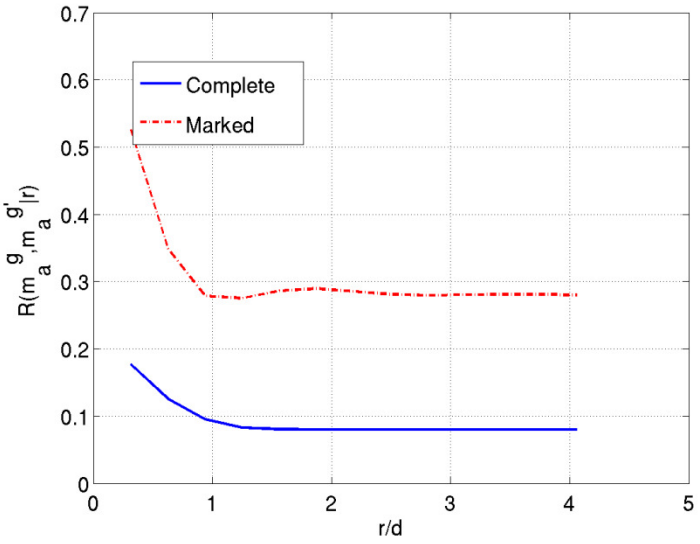

(a)

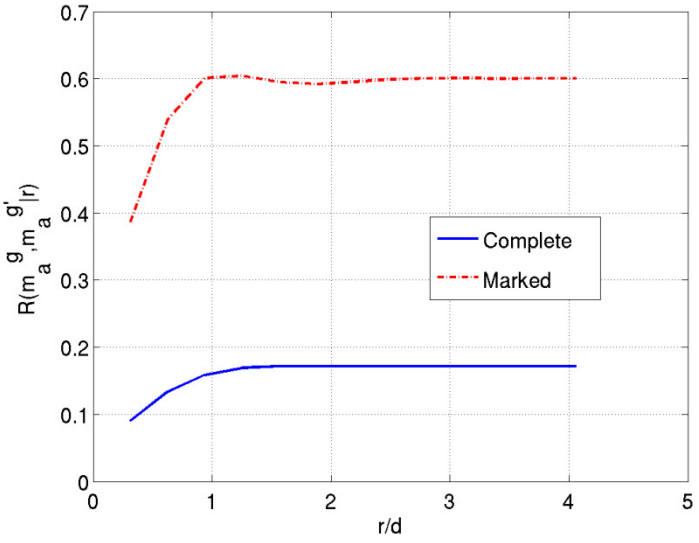

(b)

Fig. 9. For IN100 the (a) complete radial and extreme value marked radial distribution for apparent Schmid factors m_a^g =0.45 to 0.5 (cube slip) and $m_a^{g'}$ =0.45 to 0.5 (cube slip) and (b) complete radial and extreme value marked radial distribution of apparent Schmid factors m_a^g =0.45 to 0.5 (cube slip) and $m_a^{g'}$ =0.45 to 0.5 (octahedral slip) are plotted for the 100 SVEs subjected to 0.5% strain. The distance *r* that separates the two orientations is normalized against the average cube root grain size *d* (i.e., 20 μm).

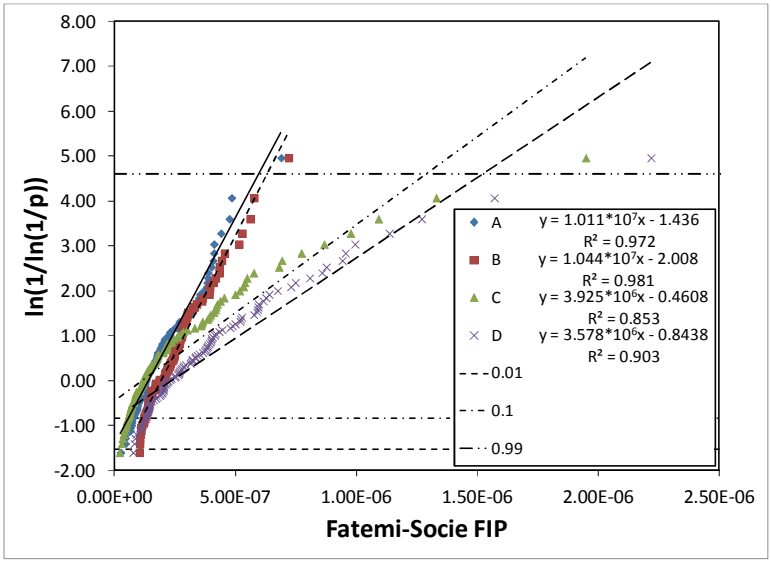

Fig. 10. The extreme value Fatemi-Socie FIP_{FS} calculated over a cube shaped averaging volume with equivalent grain size of 32 µm for the four analyzed Ti-6Al-4V microstructures plotted on Gumbel (Type I) probability scales.

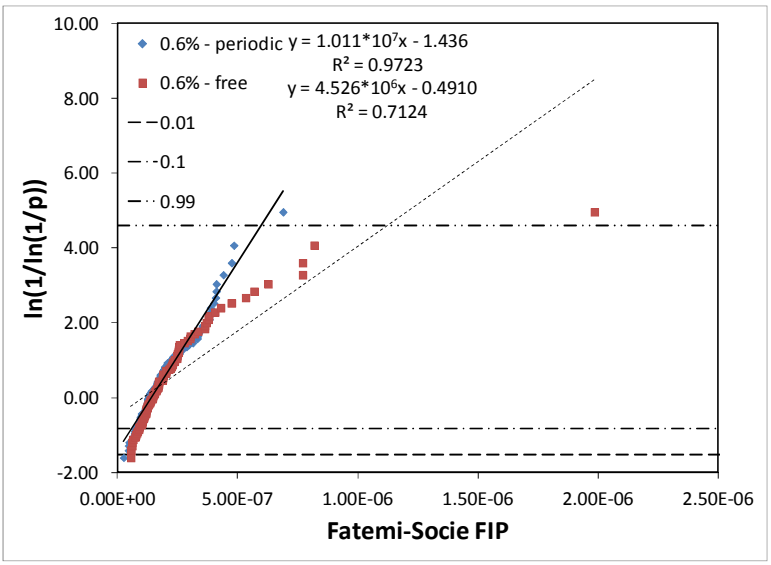

(a)

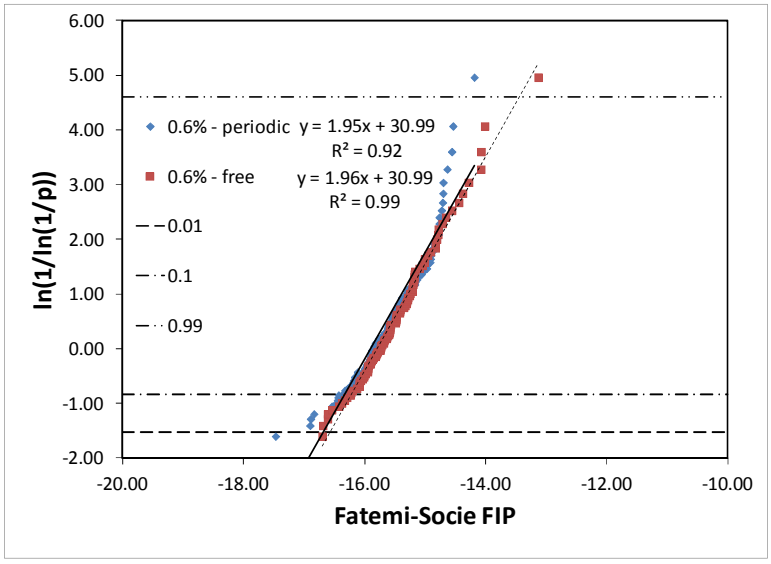

(b)

Fig. 11. The extreme value Fatemi-Socie FIP_{FS} for Ti-6Al-4V calculated over a cube shaped averaging volume with equivalent grain size of 0.032 μm for the instantiated SVEs (R_ε=0 and maximum applied strain of 0.006) with periodic BCs and with free BCs plotted on (a) Gumbel (Type I), (b) Fréchet (Type II) probability scales. The equations given for the least squares linear regression are such that $y = \ln\left(1/\ln(1/p)\right)$ and $x =$ FIP for the Gumbel probability plot and $x = ln(FIP)$ for the Fréchet probability plot, respectively.

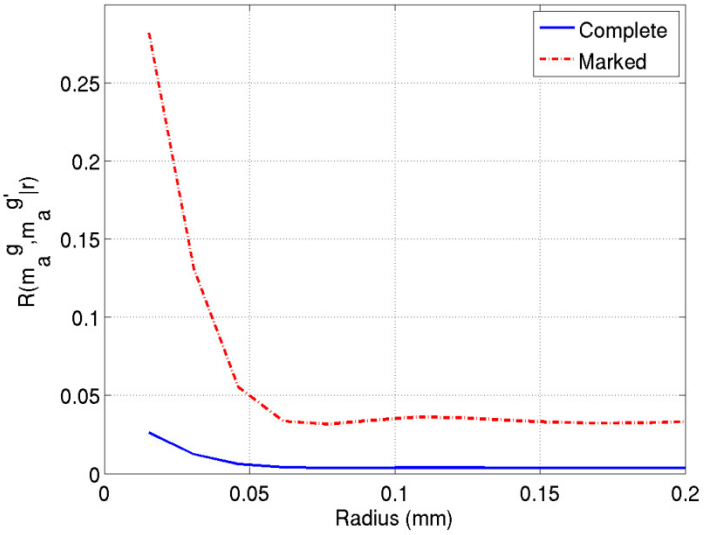

(a)

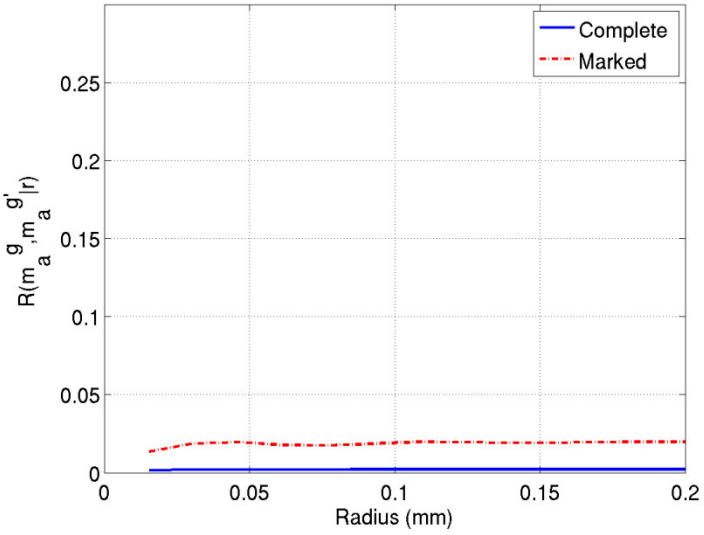

(b)

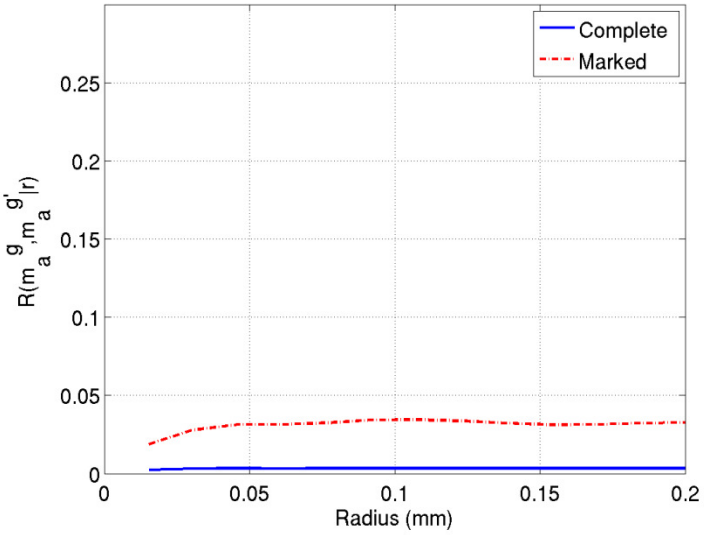

(c)

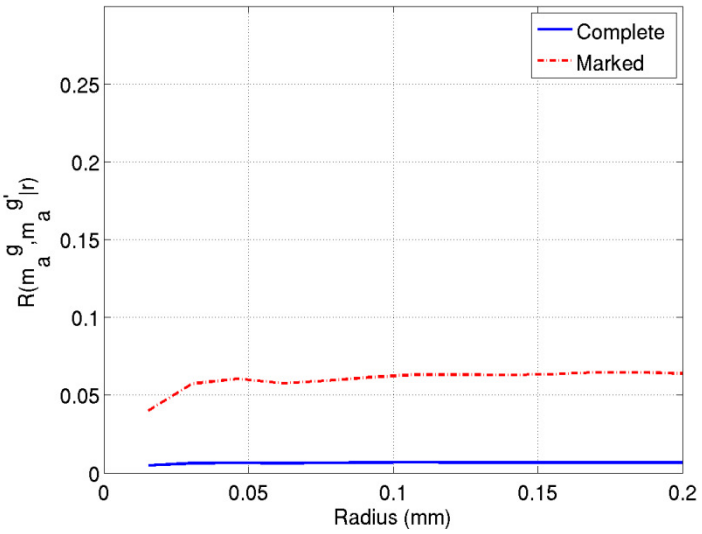

(d)

Fig. 12. Radial correlation functions for the complete Ti-6Al-4V microstructure compared with EVMCF describing the correlation between the apparent Schmid factor m_a^g for basal slip between 0.45 and 0.5 for the primary α phase and the Schmid factor $m_a^{g'}$ for: (a) basal slip between 0.45 and 0.5, (b) prismatic slip between 0.45 and 0.5, (c) pyramidal $\langle a \rangle$ slip between 0.45 and 0.5, and (d) pyramidal $\langle a+c \rangle$ slip between 0.45 and 0.5 for the primary α phase for the instantiated SVEs with fully periodic boundary conditions.

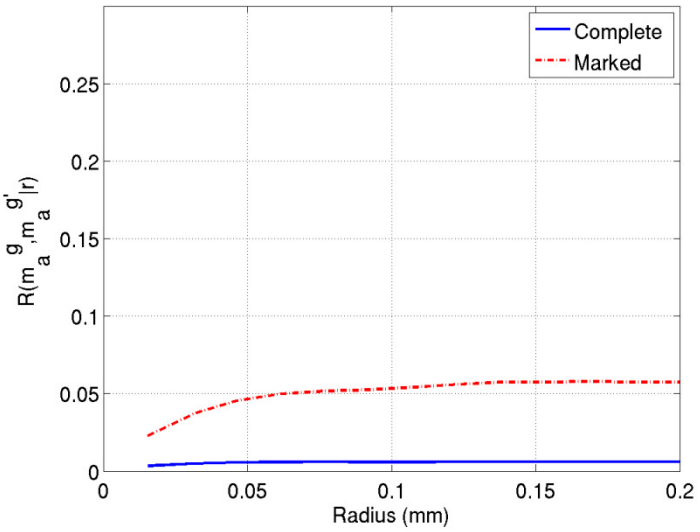

(a)

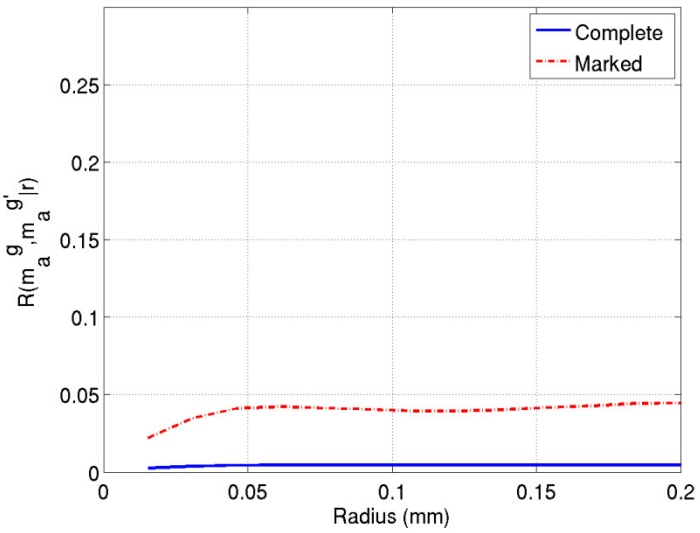

(b)

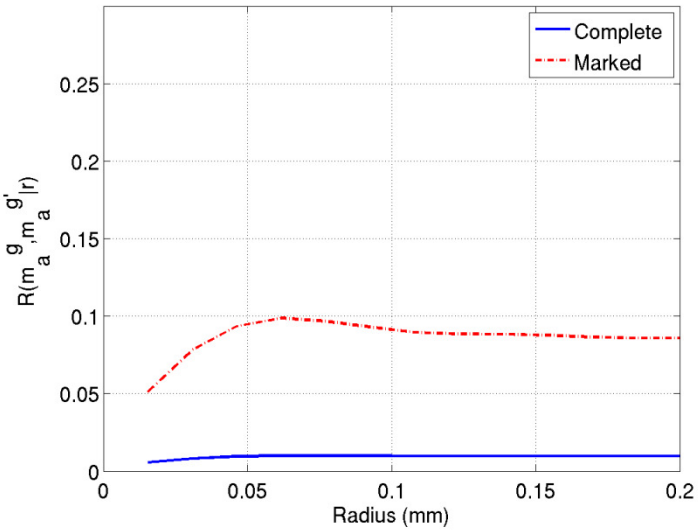

(c)

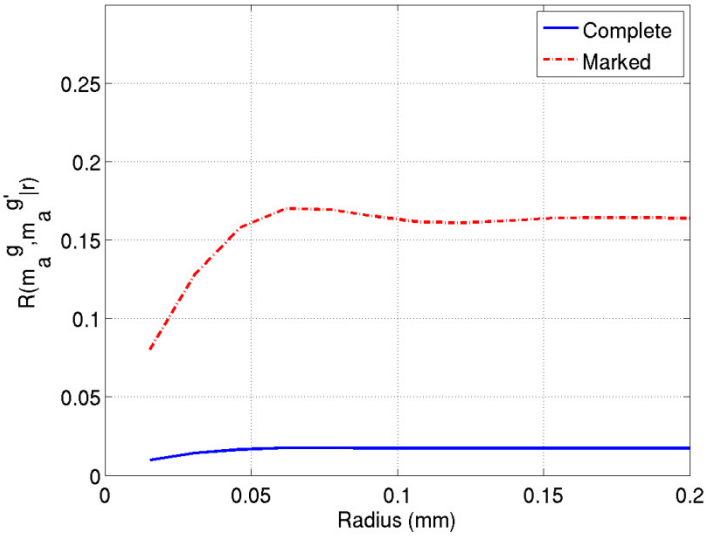

(d)

Fig. 13. Radial correlation functions for the complete microstructure compared with EVMCF describing the correlation between the apparent Schmid factor m_a^g for basal slip between 0.45 and 0.5 for the primary α phase and the apparent Schmid factor $m_a^{g'}$ for: (a) basal slip between 0.45 and 0.5, (b) prismatic slip between 0.45 and 0.5, (c) pyramidal $\langle a \rangle$ slip between 0.45 and 0.5, and (d) $\langle 111 \rangle \{110\}$ bcc slip (transformed into the hexagonal coordinate system via the BOR) between 0.45 and 0.5 for the α+β colony phase for the instantiated SVEs with fully periodic boundary conditions.

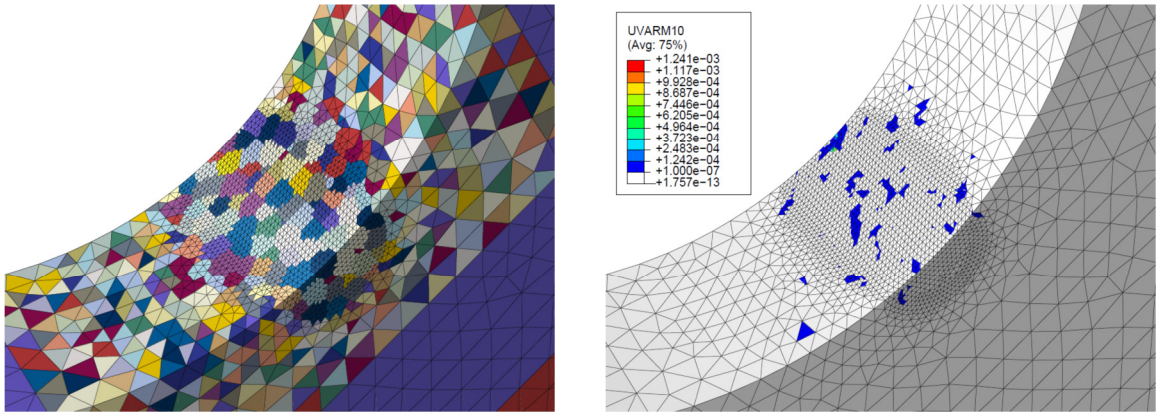

(a) Polycrystalline grain structure. (b) Effective plastic strain.

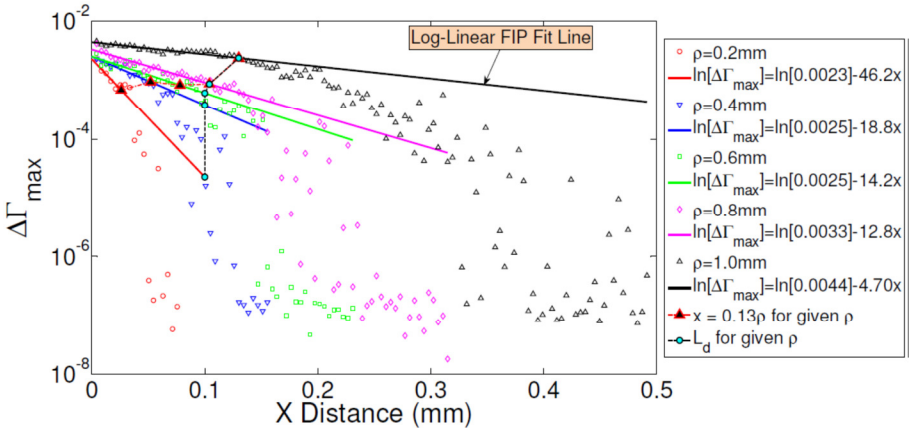

(c) FIP distribution as a function of X-distance from notch root.

Fig. 14. (a) Polycrystalline grain structure, (b) Von Mises effective plastic strain for a coarse grain IN100 notched specimen at maximum tensile load during the third fatigue cycle, $\rho = 0.6$ mm, $\varepsilon_a = 0.6\varepsilon_y$, and (c) maximum FIP distribution versus x-distance from notch root for five different notch root sizes for the coarse grain IN100 microstructure at a strain amplitude $\varepsilon_a = \varepsilon_y$.

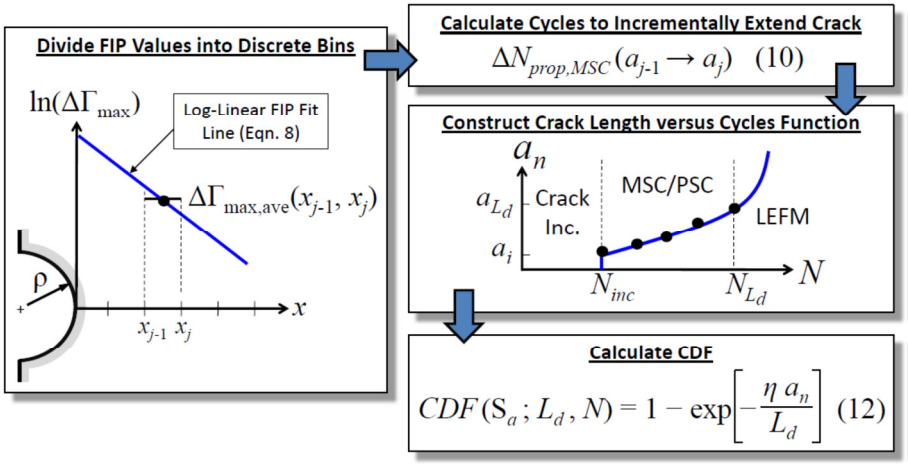

Fig. 15. Overview of method for assessing CDF for the transition crack length approach based on uncracked FIP distribution (details in Ref. [149]).

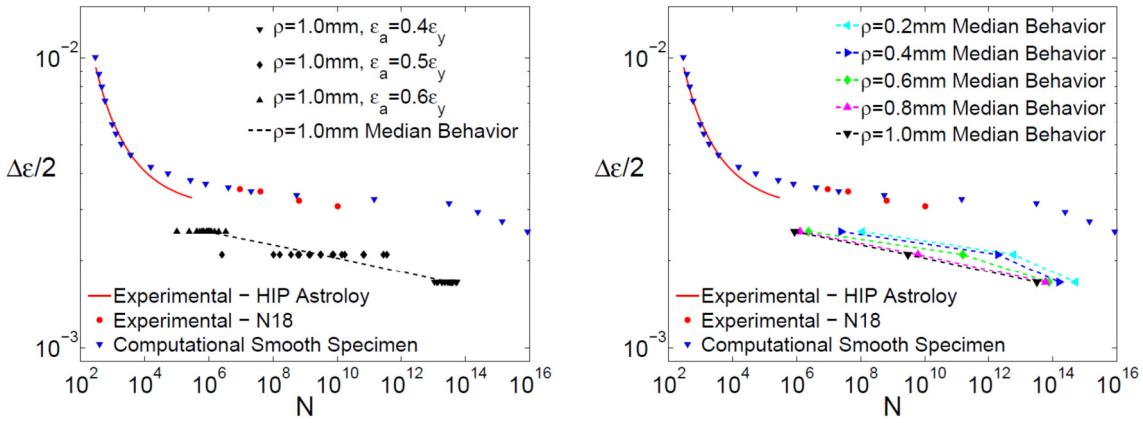

Figure 16. Comparison of coase grain IN100 smooth and notched computational strain life data versus HIP Astroloy (Cowles et al., 1978, 1980) and N18 (Bathias and Paris, 2010) smooth specimen strain-life experimental data.

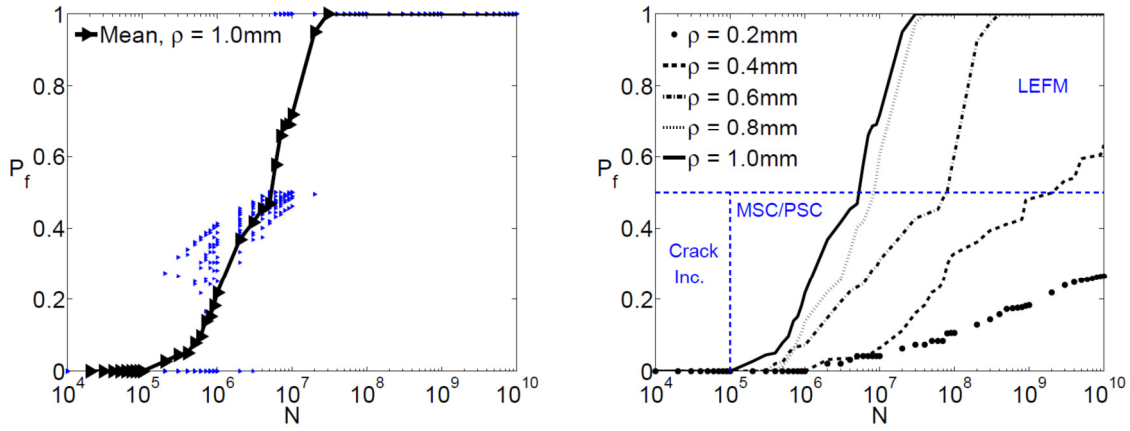

Fig. 17. Coarse grain IN100 cumulative distribution function for various notch root radii ($\varepsilon_a = 0.6\,\varepsilon_y$, $\sigma_a = 450$, $R_\varepsilon = -1$, $T = 650°C$).